Phys. Lett. B 873 (2026) 140050

Contents lists available at ScienceDirect

Physics Letters B

journal homepage: www.elsevier.com/locate/physletb

Letter

Observation of $W^+W^-\gamma$ production in pp collisions at $\sqrt{s} = 13$ TeV with the ATLAS detector and constraints on anomalous quartic gauge-boson couplings

ATLAS Collaboration[1]

ARTICLE INFO

Editor: Dr. M. Doser

Keywords:
Electroweak
Multiboson
WWgamma
Cross-section
Anomalous quartic gauge couplings
EFT

ABSTRACT

This Letter reports the observation of $W^+W^-\gamma$ triboson production in 140 fb^{-1} of data collected by the ATLAS detector from proton–proton collisions at a centre-of-mass energy of $\sqrt{s} = 13$ TeV at the LHC. Events with an opposite-charge $e\mu$ pair, a high transverse-momentum photon, and significant missing transverse momentum are considered. The observed (expected) significance of the signal is 5.9 (6.0) standard deviations. The measured fiducial cross-section, defined for the $W^+W^-\gamma \to e^\pm\mu^\mp\nu\bar{\nu}\gamma$ final state is 6.2 ± 0.8 (stat.) $\pm$ 0.6 (sys.) fb, in good agreement with the Standard Model prediction of $6.1^{+1.0}_{-0.7}$ fb. Constraints on the Wilson coefficients of 13 dimension-8 operators describing physics beyond the Standard Model through anomalous quartic gauge-boson couplings are derived using the effective field theory framework.

1. Introduction

In the Standard Model (SM), the electroweak interaction is based on the non-Abelian $SU(2)_L \times U(1)_Y$ gauge group. This leads to couplings among the electroweak gauge bosons (the W and Z bosons and the photon) through triple and quartic vertices [1]. Measurements of triboson production processes allow stringent tests of the gauge structure and offer sensitivity to physics beyond the SM.

The ATLAS [2] and CMS [3] collaborations at the Large Hadron Collider (LHC) [4] investigated both the $WW\gamma$ and $WZ\gamma$ processes [5,6] using datasets collected at a centre-of-mass energy ($\sqrt{s}$) of 8 TeV and integrated luminosities ($\mathcal{L}$) of 20.2 fb^{-1} and 19.7 fb^{-1}, respectively. The CMS Collaboration has since observed the $WW\gamma$ process at $\sqrt{s} =$ 13 TeV using its full Run-2 dataset corresponding to $\mathcal{L} = 138$ fb^{-1} [7]. Many triboson production processes have been studied by both the ATLAS and CMS collaborations using their full Run-2 datasets, including WWW [8,9], $W\gamma\gamma$ [10,11], $Z\gamma\gamma$ [11,12], $WZ\gamma$ [13,14], and WVZ, where V refers to W or Z bosons [9,15]. Both the ATLAS and CMS collaborations have set constraints on anomalous quartic gauge-boson coupling (aQGC) parameters.

This Letter reports the observation of $WW\gamma$ production by examining the $e^\pm\mu^\mp\nu\bar{\nu}\gamma$ final state in 140 fb^{-1} [16] of data from proton–proton collisions at $\sqrt{s} = 13$ TeV collected by the ATLAS detector at the LHC. Events with an opposite-charge $e\mu$ pair, a photon, and missing transverse momentum are selected. The photon in a $WW\gamma$ event can originate from three processes: direct coupling to a W boson – either triple gauge-boson coupling (TGC) or quartic gauge-boson coupling (QGC); initial-state radiation (ISR) from an initial quark; or emission as final-state radiation (FSR). In the case of FSR, the photon is emitted either by a lepton from a W boson decay or by an associated quark. Fig. 1 shows examples of the lowest-order Feynman diagrams for $WW\gamma$ production where the photon arises from a QGC vertex, a TGC vertex, or is radiated directly from a quark without involving interactions between electroweak force carriers.

The fiducial cross-section is measured using a binned maximum-likelihood fit performed on the output distribution of a boosted decision tree, which was trained to enhance the separation between signal and background. Limits on aQGCs are also derived, by performing an analysis in which deviations from the SM predictions are parameterised using effective field theory (EFT) [17].

2. ATLAS detector

The ATLAS experiment [2] at the LHC is a multipurpose particle detector with a forward–backward symmetric cylindrical geometry and nearly 4π coverage in solid angle.[1] It consists of an inner tracking de-

[1] ATLAS uses a right-handed coordinate system with its origin at the nominal interaction point (IP) in the centre of the detector and the z-axis along the beam pipe. The x-axis points from the IP to the centre of the LHC ring, and the y-axis points upwards. Cylindrical coordinates (r, ϕ) are used in the transverse plane, ϕ being the azimuthal angle around the z-axis. The pseudorapidity is defined in

Contact: atlas.publications@cern.ch.
[1] Authors are listed at the end of this paper.

https://doi.org/10.1016/j.physletb.2025.140050
Received 18 September 2025; Received in revised form 18 November 2025; Accepted 18 November 2025
Available online 29 November 2025

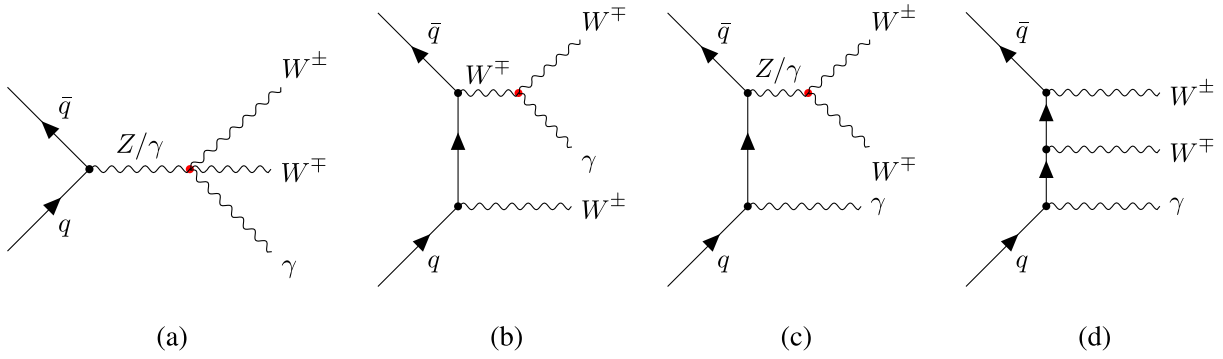

Fig. 1. Representative leading-order Feynman diagrams for the $WW\gamma$ production process with a triple or quartic gauge-boson coupling vertex shown in red: (a) diagram featuring a QGC vertex (b,c) diagrams with a TGC vertex, and (d) a diagram showing photon radiation from an initial-state quark. Additional contributions arise from other diagrams not shown here.

tector (ID) surrounded by a thin superconducting solenoid providing a 2 T axial magnetic field, electromagnetic and hadron calorimeters, and a muon spectrometer (MS). The ID covers the pseudorapidity range $|\eta| < 2.5$. It consists of silicon pixel, silicon microstrip, and transition radiation tracking detectors. Lead/liquid-argon (LAr) sampling calorimeters provide electromagnetic (EM) energy measurements with high granularity. A steel/scintillator-tile hadron calorimeter covers the central pseudorapidity range ($|\eta| < 1.7$). The endcap and forward regions are instrumented with LAr calorimeters for both the EM and hadronic energy measurements up to $|\eta| = 4.9$. The MS surrounds the calorimeters and is based on three large superconducting air-core toroidal magnets with eight coils each. The field integral of the toroids ranges between 2.0 and 6.0 T · m across most of the detector. The muon spectrometer includes a system of precision chambers for tracking and fast detectors for triggering. A two-level trigger system is used to select events. The first-level trigger is implemented in hardware and uses a subset of the detector information to accept events at a rate below 100 kHz. This is followed by a software-based trigger that reduces the accepted event rate to 1.25 kHz on average depending on the data-taking conditions. A software suite [18] is used in data simulation, in the reconstruction and analysis of real and simulated data, in detector operations, and in the trigger and data acquisition systems of the experiment.

3. Data and MC simulation

This measurement uses 140 fb^{-1} of $\sqrt{s} = 13$ TeV proton–proton collision data collected by the ATLAS detector from 2015 to 2018 [16]. The selected data were collected during periods with stable LHC beam conditions and a fully functioning ATLAS detector [19]. Events were required to satisfy a single-electron or single-muon trigger [20,21]. Single-lepton triggers with low transverse momentum (p_{T}) thresholds and isolation requirements were combined with triggers applying higher p_{T} thresholds, looser identification criteria, and no isolation requirements, resulting in an efficiency of almost 100 % for events satisfying the analysis selection criteria. The lowest p_{T} threshold ranged from 24 GeV to 26 GeV for single-electron triggers and from 20 GeV to 26 GeV for single-muon triggers. The average number of collisions per bunch crossing (pile-up) ranged from 13 to 38 during the 2015–2018 data-taking periods.

Monte Carlo (MC) simulated event samples are used to model the signal and irreducible backgrounds. The MC events were passed through a GEANT4-based simulation of the ATLAS detector [22,23] to account for detector resolution and acceptance effects. For some samples used in the evaluation of systematic uncertainties, a faster parameterised shower simulation was employed in place of the full GEANT4 model. Inelastic collisions were simulated using the PYTHIA 8.186 [24] MC event generator with the A3 set of tuned parameters [25] and the NNPDF2.3LO [26] set of parton distribution functions (PDFs) and overlaid on simulated signal and background events. Correction factors are applied to account for differences between data and simulation in the amount of pile-up and in the reconstruction, particle identification, and trigger efficiencies.

Signal $WW\gamma$ events including up to two light-flavour jets were generated using SHERPA 2.2.11 [27] and the NNPDF3.0NNLO PDF set [28], together with the default SHERPA tuning of parton-shower parameters. The $WW\gamma$ + 0-jet events were simulated at next-to-leading order (NLO) in QCD, and combined with $WW\gamma$ + 1-jet and $WW\gamma$ + 2-jet event samples, which were simulated at leading order (LO) using matrix elements from the Comix [29] and OPENLOOPS [30–32] libraries. The partons were matched with the SHERPA parton shower [33] using the ME + PS@NLO prescription [34–37] with the set of tuned parameters developed by the SHERPA authors. The $WW\gamma$ process was simulated in the $\ell\nu\ell\nu\gamma$ ($\ell = e, \mu, \tau$) final state, including contributions from off-shell W bosons and lepton pairs not originating from W boson decays such as $ZZ\gamma \to \ell\ell\nu\nu\gamma$. Photons radiated from initial- or final-state charged particles were included. A minimum photon energy of 7 GeV and a separation of $\Delta R > 0.1$ between the photon and charged leptons were required. Processes with a b-quark in the initial or final state are excluded because they are dominated by top-quark contributions rather than diagrams with gauge-boson couplings. This procedure also removes small $b\bar{b}$-induced signal contributions that are free of top quarks, but the impact on the total cross-section is less than 1 %, as evaluated with SHERPA for $WW\gamma$ + 0-jet production at LO in QCD.

For the EFT interpretation described in Section 9, MC samples were generated with non-zero Wilson coefficients for the $\mathcal{O}_{\mathrm{M0}}$, $\mathcal{O}_{\mathrm{M1}}$, $\mathcal{O}_{\mathrm{M2}}$, $\mathcal{O}_{\mathrm{M3}}$, $\mathcal{O}_{\mathrm{M4}}$, $\mathcal{O}_{\mathrm{M5}}$, $\mathcal{O}_{\mathrm{M7}}$, $\mathcal{O}_{\mathrm{T0}}$, $\mathcal{O}_{\mathrm{T1}}$, $\mathcal{O}_{\mathrm{T2}}$, $\mathcal{O}_{\mathrm{T5}}$, $\mathcal{O}_{\mathrm{T6}}$, and $\mathcal{O}_{\mathrm{T7}}$ operators in the Eboli model [17] at LO in QCD using MADGRAPH5_AMC@NLO 2.9.9 [38], interfaced with PYTHIA 8.3, and employing the NNPDF3.0NNLO PDF set. These samples include only on-shell W bosons and no additional partons in the matrix element (ME). The Wilson coefficients were set to 1 TeV^{-4} in all EFT samples. In addition, a SM $WW\gamma$ event sample was generated using the same MADGRAPH5_AMC@NLO + PYTHIA setup. The ratio of SHERPA to MADGRAPH5_AMC@NLO SM predictions was used to derive $p_{\mathrm{T}}(\gamma)$-dependent corrections for the EFT samples, with a correction factor of approximately 2.3 observed in the high-$p_{\mathrm{T}}(\gamma)$ region, $p_{\mathrm{T}}(\gamma) > 500$ GeV.

Simulated event samples containing prompt photons and leptons are used to model background processes with final states similar to the signal. These include $t\bar{t}\gamma$, $tW\gamma$, $Z\gamma$, $WZ\gamma$ and $ZZ\gamma$ productions.

MC $t\bar{t}\gamma$ background events with photons from ISR were generated at NLO in QCD with MADGRAPH5_AMC@NLO 2.7.3 [38] using the NNPDF3.0NLO PDF set [28] interfaced to PYTHIA 8.240 [39], which

terms of the polar angle θ as $\eta = -\ln\tan(\theta/2)$. Angular distance is measured in units of $\Delta R \equiv \sqrt{(\Delta\eta)^2 + (\Delta\phi)^2}$.

used the A14 set tune [40] and the NNPDF2.3LO PDF set for the parton shower (PS). Top quarks were decayed at LO in QCD using MadSpin [41,42]. With the same setup, a second $t\bar{t}\gamma$ sample with photons from FSR was generated as a $2 \to 2$ process with on-shell top quarks at LO precision, where the photon originates from the charged decay products of the top quarks. The normalisation of this sample is corrected by a NLO/LO inclusive k-factor of 1.5 obtained in Ref. [43]. The production of $tW\gamma$ was simulated at LO in QCD with MadGraph5_aMC@NLO interfaced to Pythia 8.212 using the A14 tune and the NNPDF2.3LO PDF set. Two samples were generated: one where the photon originates from the initial state or from radiative tW production, and another where the photon arises from the decay of the top quark, the W boson, or their charged decay products.

The $Z\gamma$ MC event sample was generated as $\ell\ell\gamma$ ($\ell = e, \mu, \tau$) with Sherpa 2.2.8 [27]. The $Z\gamma$ events with two or three light-flavour jets were simulated at LO in QCD, whereas $Z\gamma$ + 0,1-jet events were simulated at NLO in QCD. Background $WZ\gamma$ and $ZZ\gamma$ (referred to as $VZ\gamma$) MC events were generated at NLO in QCD as $\ell\nu\ell\ell\gamma$ and $\ell\ell\ell\ell\gamma$ ($\ell = e, \mu, \tau$) final states with Sherpa 2.2.11. Those with one or two additional light-flavour jets were simulated at LO in QCD and combined with the $WZ\gamma$ + 0-jet and $ZZ\gamma$ + 0-jet NLO samples. The NNPDF3.0nnlo PDF set [28] was used for these samples. Events with off-shell W or Z bosons were included, as were those with a photon radiated from an initial- or final-state charged particle.

Background events in which at least one lepton or photon is not prompt or is due to misidentification, referred to as fake-lepton and fake-photon backgrounds, can also mimic the signal. These contributions are estimated using MC samples, with their normalisation and shape corrected using data-driven methods and dedicated control regions. The contributing processes include diboson (VV), $t\bar{t}$, tW and Z + jets production.

The diboson samples were generated with Sherpa 2.2.12 using the same setup as the signal, i.e. the NNPDF3.0nnlo PDF set and the dedicated parton-shower tuning provided by the Sherpa authors. The $t\bar{t}$ and tW event samples were generated at NLO in QCD with Powheg Box v2 [44–47] with the NNPDF3.0nlo PDF set and the h_{damp} parameter[2] set to $1.5\, m_{\text{top}}$ [48]. Both samples were interfaced to Pythia 8.230 [39], which used the A14 tune and the NNPDF2.3LO PDF set. The Z + jets MC sample was generated with Sherpa 2.2.1 [27], using NLO QCD matrix elements for up to two partons and LO QCD matrix elements for three or four partons, together with the NNPDF3.0nnlo PDF set.

4. Object reconstruction and event selection

A primary vertex [49] is constructed by requiring at least two tracks consistent with a pp collision at the interaction point. The primary vertex with the highest sum of the squared transverse momenta of all associated tracks with $p_{\text{T}} > 500$ MeV is selected.

Electron candidates are reconstructed from energy clusters in the EM calorimeter and matched to reconstructed tracks in the ID [50,51]. Electrons are also required to meet the `TightLH` identification and `PLVTight` isolation criteria, and to satisfy $p_{\text{T}} > 20$ GeV and $|\eta| < 2.47$, excluding the transition region $1.37 < |\eta| < 1.52$ between the calorimeter barrel and endcaps. Electron tracks must also be consistent with originating from the primary vertex by satisfying $|d_0|/\sigma_{d_0} < 5$ and $|z_0 \cdot \sin\theta| < 0.5$ mm. Here, d_0 denotes the transverse impact parameter with respect to the beamline, σ_{d_0} is its associated uncertainty, z_0 is the longitudinal impact parameter with respect to the primary vertex, and θ is the polar angle of the track.

Photon candidates are reconstructed from energy clusters in the EM calorimeter [50]. Photon energy clusters must be within $|\eta| < 2.37$, excluding the transition region $1.37 < |\eta| < 1.52$ between the barrel and endcaps. Photon candidates are required to meet the `Tight` identification and `FixedCutTight` isolation criteria and have $p_{\text{T}} > 20$ GeV [50].

Muon candidates are reconstructed by combining a track reconstructed in the ID with one reconstructed in the MS [52] and are required to have $p_{\text{T}} > 20$ GeV and $|\eta| < 2.5$. Several quality requirements are imposed to reject non-prompt muon candidates, which originate primarily from pion and kaon decays. Muons are required to meet `Medium` identification and `Tight` isolation criteria [52]. Muon tracks are also required to be consistent with originating from the primary vertex by satisfying $|d_0|/\sigma_{d_0} < 3$ and $|z_0 \cdot \sin\theta| < 0.5$ mm.

Jet-related variables play an important role in this analysis. A veto on jets originating from b-quarks (b-jets) is primarily used to suppress backgrounds from top-quark processes, and additional jet-related observables are used in the boosted decision tree to enhance signal–background separation. Jets are reconstructed from particle-flow objects [53], using the anti-k_t algorithm [54,55] with a radius parameter of $R = 0.4$. Jets are required to have $p_{\text{T}} > 20$ GeV and $|\eta| < 2.5$. Jets with $p_{\text{T}} < 60$ GeV and $|\eta| < 2.5$ must fulfil the requirement of a likelihood tagger called the Jet Vertex Tagger (`JVT`) to reduce the impact of pile-up [56]. A `JVT` requirement that has 92 % efficiency while rejecting 98 % of jets from pile-up and noise is imposed. Identification of b-jets is based on reconstructing secondary vertices formed by tracks associated with jets and combining their spatial-parameter values with lifetime-related information. The `DL1r` b-tagging algorithm [57–59] is used at a working point with an 85 % b-jet-tagging efficiency, independent of b-jet p_{T} and calibrated using simulated $t\bar{t}$ events. The rejection rates for light-flavour jets and c-jets are p_{T}-dependent, and on average are 40 and 3, respectively.

The missing transverse momentum, $E_{\text{T}}^{\text{miss}}$, provides a measure of the transverse momentum imbalance due to escaping neutrinos. The $E_{\text{T}}^{\text{miss}}$ is calculated as the magnitude of the negative vector sum of the transverse momenta of all reconstructed electrons, muons, photons, and jets in the event, plus a term to account for soft hadronic activity, built from tracks associated with the hard-scattering vertex but not matched to any of the reconstructed objects [60].

Object reconstruction is followed by an overlap removal procedure applied to electrons, photons, muons and jets to remove possible duplication due to individual physical objects being reconstructed as two different entities in the detector [61].

The $WW\gamma$ process yields several different final states depending on the decay modes of the W bosons. In this measurement, the targeted final state contains an electron and a muon of opposite electric charge, accompanied by missing transverse momentum and exactly one photon. This selection defines the $e^{\pm}\mu^{\mp}\nu\bar{\nu}\gamma$ signal region (SR). The $e^{\pm}\mu^{\mp}\nu\bar{\nu}\gamma$ final state, together with a veto on events containing b-jets, is chosen in order to suppress background contributions, particularly from $t\bar{t}\gamma$, $Z\gamma$, and $tW\gamma$ production. Throughout this analysis, ℓ refers exclusively to electrons or muons.

Events must have exactly one muon and one electron satisfying the requirements described above. At least one lepton must have $p_{\text{T}} > 27$ GeV to satisfy the trigger threshold, and be matched to the lepton that was accepted by the trigger. Exactly one photon is required, meeting the identification and isolation requirements specified previously. In addition, events are required to have $E_{\text{T}}^{\text{miss}} > 20$ GeV. A Z-boson veto is applied mainly to reduce contributions from $WZ \to \mu^{\pm}\nu e^{+}e^{-}$, where one electron from the $Z \to e^{+}e^{-}$ decay is reconstructed as a prompt photon. This is achieved by requiring $|m(e\gamma) - m_Z| > 5$ GeV. Additionally, events containing b-jets are vetoed to reduce $t\bar{t}\gamma$ and $tW\gamma$ background contributions. These signal event requirements are summarised in Table 1.

5. Background estimation

The background yields are estimated using a combination of MC simulations and data-driven methods, and are constrained using statistically

[2] The h_{damp} parameter is a resummation damping factor and one of the parameters that controls the matching of the Powheg Box ME to the PS and thus effectively regulates the high-p_{T} radiation against which the $t\bar{t}$ system recoils.

Table 1
Signal and control regions used in the analysis. The Z-boson mass m_Z is taken to be 90 GeV. Selections shown in boldface correspond to differences with respect to the SR, chosen both to enhance the targeted background and to ensure orthogonality between regions.

Common selections				
Leading lepton $p_{\mathrm{T}} > 27$ GeV Subleading lepton $p_{\mathrm{T}} > 20$ GeV Exactly 1 photon with $p_{\mathrm{T}} > 20$ GeV $E_{\mathrm{T}}^{\mathrm{miss}} > 20$ GeV				
SR $e^{\pm}\mu^{\mp}\nu\bar{\nu}\gamma$	CR $t\bar{t}\gamma$	CR1 $Z\gamma$	CR2 $Z\gamma$	CR $e \to \gamma$
$e^{\pm}\mu^{\mp}$	$e^{\pm}\mu^{\mp}$	$\boldsymbol{e^+e^-/\mu^+\mu^-}$	$\boldsymbol{e^+e^-/\mu^+\mu^-}$	$e^{\pm}\mu^{\mp}$
$\lvert m(e\gamma) - m_Z\rvert > 5$ GeV	$\lvert m(e\gamma) - m_Z\rvert > 5$ GeV	–	–	$\boldsymbol{\lvert m(e\gamma) - m_Z\rvert < 5\,\mathrm{GeV}}$
–	–	$\boldsymbol{m(\ell\ell\gamma) < 100\,\mathrm{GeV}}$	$\boldsymbol{m(\ell\ell\gamma) > 100\,\mathrm{GeV}}$	–
0 b-jets	**1 b-jet**	0 b-jets	0 b-jets	0 b-jets

independent control regions (CRs). Table 1 summarises the event selection criteria and defines the CRs used to estimate the normalisation of the major backgrounds.

The modelling of prompt backgrounds, such as those due to the $t\bar{t}\gamma$ and $Z\gamma$ processes, is based on MC simulations, with their normalisations determined by a maximum-likelihood fit using dedicated $t\bar{t}\gamma$ and $Z\gamma$ CRs. The $t\bar{t}\gamma$ CR matches the kinematic properties of the signal region, but requires exactly one b-jet. Two $Z\gamma$ CRs are constructed, each selecting $\ell\ell\gamma$ events with a $e^+e^-/\mu^+\mu^-$ lepton pair. The $Z\gamma$ CR1 requires $m(\ell\ell\gamma) < 100$ GeV, whereas $Z\gamma$ CR2 requires $m(\ell\ell\gamma) > 100$ GeV, resulting in an approximately 30 % contribution from jets or neutral hadrons misidentified as photons ($j \to \gamma$), making it well suited to constrain this background. An additional control region (the $e \to \gamma$ CR) is defined by requiring $|m_{e\gamma} - m_Z| < 5$ GeV, in order to constrain backgrounds from electrons misidentified as photons ($e \to \gamma$). This region is dominated by WZ events, where an electron from the Z-boson decay is reconstructed as a photon.

These $j \to \gamma$ background events stem from processes without prompt photons, typically $t\bar{t}$, Z + jets, or diboson (VV), where jets occasionally satisfy the photon identification and isolation criteria. Samples of MC events from these processes are used to estimate the $j \to \gamma$ misidentification background. An overlap-removal procedure ensures orthogonality between prompt- and non-prompt-photon MC samples [62]. Events with photons from initial- or final-state radiation (ISR/FSR) are included in prompt-photon samples (e.g. $t\bar{t}\gamma$), while jet-induced photon-like objects remain in non-prompt-photon samples (e.g. $t\bar{t}$). Discrepancies between MC simulation and data are minimised by applying two-dimensional scale factors (SFs) derived as functions of the scalar sum of jet transverse momenta, Σp_{T}(jet), and the transverse mass of the dilepton–$E_{\mathrm{T}}^{\mathrm{miss}}$ system, $m_{\mathrm{T}}(\ell\ell, E_{\mathrm{T}}^{\mathrm{miss}})$. The use of these variables, sensitive to event kinematics and the presence of jets and leptons, effectively addresses modelling mismatches.

The correction SFs are calculated in a statistically independent region enriched in $j \to \gamma$ events, where SR selection requirements other than the photon isolation criterion are applied. The photon candidate fails the `FixedCutTight` isolation requirement [50], but passes a looser selection, in which the sum of track p_{T} within a cone of $\Delta R = 0.2$ around the photon is less than 5 % of $p_{\mathrm{T}}(\gamma)$, and the calorimeter-based isolation requirement is reversed. This region is kinematically similar to the SR, allowing the scale factors to be applied reliably. The SFs are computed by normalising the $j \to \gamma$ MC event yields to data after subtracting contributions from prompt backgrounds. The resulting scale factors typically range between 0.8 and 1.5. The associated uncertainties, arising from limited numbers of data and MC events, range from ±0.2 to ±0.7 and are treated as additional systematic uncertainties.

The $j \to \gamma$ background estimate is cross-checked using a two-dimensional sideband technique [10]. Four non-overlapping regions are defined by using two uncorrelated variables: photon identification and photon isolation. The SR requires photons to satisfy both the `Tight` identification and the `FixedCutTight` isolation criteria. Three CRs are constructed by inverting the identification and/or isolation criteria to enhance the contribution from misidentified jets. This is done by selecting events with a photon candidate that passes the `Loose` photon identification requirement but fails at least two of the EM shower-shape requirements used in `Tight` identification; these photons are denoted by T'. For isolation (I), the photon candidate must pass the track-isolation requirement but fail the calorimeter-isolation requirement (I'). The $j \to \gamma$ yield in the SR is then estimated as $TI = T'I \cdot TI'/T'I'$. As an additional cross-check, the procedure is repeated with photon identification paired with the requirement of same-sign lepton events instead of the $e^{\pm}\mu^{\mp}$ selection. The two $j \to \gamma$ estimates, obtained from the sideband and scale-factor methods, differ by 30 %, which is assigned as an additional systematic uncertainty on the $j \to \gamma$ background in the SR.

Backgrounds such as diboson events with electron-to-photon ($e \to \gamma$) misidentification are significantly suppressed by rejecting events with $m(e\gamma)$ within the Z-boson mass window. The remaining $e \to \gamma$ "fake rate" is estimated using a data-driven reweighting method, as described in Refs. [10,63]. The rate estimate is derived from $Z \to e^+e^-$ events reconstructed as $e\gamma$ final states, using two dedicated regions. An $e\gamma$ region is defined by requiring one electron and one photon with an invariant mass within 35 GeV of the Z-boson mass, and the photon p_{T} to be less than the electron p_{T} (to make the photon more likely to be fake). An e^+e^- region is defined by selecting events with two oppositely charged electrons with an invariant mass within 35 GeV of the Z-boson mass. In both regions, events containing b-jets are removed.

The invariant mass distributions in the $e\gamma$ and e^+e^- control regions are modelled using a single-sided Crystal Ball function [64] for the Z-boson resonance and a fifth-order Bernstein polynomial for non-resonant background processes. The yields $N_{e\gamma}$ and N_{ee} are binned in p_{T} and $|\eta|$ of the fake photon, and fake-factors are then defined as the ratio $N_{e\gamma}/N_{ee}$. The correction scale factors, typically between 0.71 and 1.26, are derived as the MC-to-data ratio of the fake-factors, and are used to reweight MC samples that include $e \to \gamma$ misidentification events. A systematic uncertainty is assigned to account for the limited number of data and MC events used in the evaluation of the scale factors, ranging from ±0.01 to ±0.21. An additional background uncertainty is included to account for the choice of parameterisation.

Finally, contributions from fake leptons are found to be negligible in the regions considered. Photon contributions from pile-up are evaluated following the method described in Ref. [65] and are found to be well modelled in the MC simulation, with no additional treatment required.

The predicted yield of $WW\gamma$ events in the SR after the likelihood fit (post-fit) is 250 ± 40, constituting 26 % of the expected total number of events. The quoted uncertainty includes both statistical and systematic components from the likelihood fit to data, as described in Section 8. Most of the background in the $e^{\pm}\mu^{\mp}\nu\bar{\nu}\gamma$ SR comes from sources with prompt photons, including $t\bar{t}\gamma$ (45 %), $Z\gamma$ (13 %) and $VZ\gamma$ (3 %). The

Table 2
Input variables used to train the BDT in the $e^{\pm}\mu^{\mp}\nu\bar{\nu}\gamma$ SR, ordered by feature importance. For jet-related observables, values are set to −99 if the required number of jets is not reconstructed: $\Delta R(jj)$ and $p_{\mathrm{T}}(j_2)$ for fewer than two jets, and $p_{\mathrm{T}}(j_1)$ for zero jets.

Variable	Feature importance	Definition
$m_{\mathrm{T}}(\ell_1, E_{\mathrm{T}}^{\mathrm{miss}})$	13 %	Transverse mass of the leading lepton and $E_{\mathrm{T}}^{\mathrm{miss}}$.
$\Delta R(jj)$	11 %	ΔR between the leading and subleading jets.
$m(\ell\ell)$	11 %	Invariant mass of the two-lepton system in the event.
$p_{\mathrm{T}}(j_2)$	11 %	p_{T} of the subleading jet.
$\Sigma\lvert p_{\mathrm{T}}(j)\rvert$	10 %	Scalar sum of the p_{T} of all jets in the event.
$m_{\mathrm{T}}(\ell_2, E_{\mathrm{T}}^{\mathrm{miss}})$	10 %	Transverse mass of the subleading lepton and $E_{\mathrm{T}}^{\mathrm{miss}}$.
$p_{\mathrm{T}}(j_1)$	10 %	p_{T} of the leading jet.
N(jets)	9 %	Number of jets in the event.
$\Sigma\lvert p_{\mathrm{T}}(\ell)\rvert$	9 %	Scalar sum of the p_{T} of the two leptons in the event.
$m(\ell_2\gamma)$	6 %	Invariant mass of the subleading lepton and photon.

remaining background contributions are due to non-prompt or misidentified photons, and include events where an electron is misidentified as a photon ($e \to \gamma$, 3.5 %) and events where a jet is misidentified as a photon ($j \to \gamma$, 9.5 %).

6. Multivariate analysis

To improve the separation between signal and background events, the `XGBoost` [66] package is used to train a boosted decision tree (BDT), which constructs a discriminant that takes correlations among the input variables into account, resulting in a single continuous output variable in the interval $[0, 1]$. The BDT is implemented with hyperparameters optimised for performance and stability, using 120 trees with a maximum depth of four.

The BDT is trained using MC events from the SR, where all signal and background processes are included in the training and weighted according to their expected event yields. The $e \to \gamma$ and $j \to \gamma$ backgrounds are scaled using the MC correction scale factors described in Section 5. A 5-fold cross-validation strategy [67,68] is used to improve the statistical stability of the trained BDT by training five independent models. The resulting BDT output distributions from the five held-out sets are added to form the final BDT distribution used in the statistical fit.

Only variables that provide good signal-background separation and are well modelled are used in the BDT training. The ten input variables with the highest feature importance are selected, and the full list is shown in Table 2. The feature importance is calculated using the Gain method [66].

The distributions of the four variables contributing the most to the BDT, shown after the likelihood fit described in Section 8, are presented in Fig. 2. The jet-related variables provide good separation between the $WW\gamma$ and $t\bar{t}\gamma$ processes. In contrast, the remaining BDT input variables provide discrimination power between the signal and the $Z\gamma$ and $VZ\gamma$ backgrounds.

7. Systematic uncertainties

Systematic uncertainties related to the efficiency of reconstructing the $WW\gamma$ signal and major backgrounds, and the normalisation of the $VZ\gamma$ background contribution, are taken into account. Experimental and theoretical uncertainties affecting the kinematic distributions used in the analysis are also included, with correlations across the analysis regions applied.

Reconstruction efficiency and calibration uncertainties: Systematic uncertainties affecting the reconstruction efficiency, energy calibration, and identification of electrons, photons, muons and jets are propagated through the analysis. Each source contributes only at the few-percent level to the total uncertainty in the measured signal cross-section.

Differences between electron (muon) trigger, reconstruction and selection efficiencies in data and those in MC simulation are minimised by applying scale factors derived from dedicated $Z \to e^+e^-$ ($Z \to \mu^+\mu^-$) enriched control samples using a tag-and-probe method [50,52]. Similarly, corrections and associated uncertainties for photon reconstruction and identification efficiencies are derived as described in Ref. [50].

The jet energy scale (JES) was derived using test-beam data, LHC collision data, and simulation information. The JES calibration [69] includes corrections that account for detector problems, jet fragmentation, the impact of pile-up, and differences between data and MC simulation. The impact of the uncertainty in the jet energy resolution (JER) [69] is evaluated by smearing the jet energy in the MC and data samples accordingly. An additional uncertainty arises from the correction applied to simulated events associated with the JVT selection [70].

The b-tagging efficiencies and mistagging rates are measured in data as described in Refs. [57,58,71], with the systematic uncertainties associated with the b-tagging efficiency and the mistagging rates estimated separately. The impact of the uncertainties in the b-tagging calibration is evaluated separately for b-jets, c-jets and light-flavour jets in the MC samples.

E_T^{miss}: The uncertainty in $E_{\mathrm{T}}^{\mathrm{miss}}$ due to a possible miscalibration of the soft-track component of the $E_{\mathrm{T}}^{\mathrm{miss}}$ is derived from data–MC comparisons of the p_{T} balance between the hard and soft $E_{\mathrm{T}}^{\mathrm{miss}}$ components [60]. The uncertainties associated with the leptons, jets and photons are propagated from their energy/momentum scale and resolution uncertainties, and are grouped with other uncertainties associated with those objects.

Luminosity: The uncertainty in the combined 2015–2018 integrated luminosity is 0.83 % [16], obtained using the LUCID-2 detector [72] for the primary luminosity measurements.

Uncertainty in pile-up modelling: The uncertainty in pile-up modelling is accounted for by varying the reweighting of the MC samples to the data pile-up conditions by the uncertainty in the average number of interactions per bunch crossing.

Signal and background modelling: The systematic uncertainties in the $WW\gamma$ and $Z\gamma$ modelling are estimated using the internal SHERPA 2.2.11 weights. These correspond to independently varying the renormalisation scale (μ_{r}) up and down by a factor of 2 while keeping μ_{f} fixed, and vice versa for the factorisation scale (μ_{f}). The PDF uncertainties are estimated using the nominal and variation weights provided for the PDF4LHC PDF set [73]. The resulting uncertainty is applied to the nominal signal sample. The uncertainty from the strong coupling constant, α_{s}, is evaluated for the $WW\gamma$ process, using the NNPDF3.0 PDF set with varied α_{s} values. The variations in μ_{r}, μ_{f}, the PDFs, and α_{s} are applied simultaneously to both the matrix-element calculation and the parton shower.

The systematic uncertainties associated with the renormalisation and factorisation scales of the $t\bar{t}\gamma$ and $tW\gamma$ processes are estimated by raising and lowering μ_{r} and μ_{f} by a factor of 2 in MADGRAPH5_AMC@NLO. The PDF uncertainties are evaluated with the NNPDF2.3LO PDF set [26] following the PDF4LHC prescription [73]. The systematic uncertainty associated with the parton shower and hadronisation modelling is estimated by comparing samples generated with MADGRAPH5_AMC@NLO 2.3.3 and interfaced with either PYTHIA 8.212 or HERWIG 7. For the $t\bar{t}\gamma$ process, an additional systematic uncertainty due to initial- and final-state radiation modelling and α_{s} is estimated by varying the "Var3c" parameter [40] in the A14 tune of PYTHIA 8.

Data-driven background: For the $j \to \gamma$ background, a systematic uncertainty is included to account for the limited numbers of data and MC events in the regions used to derive the estimate. This uncertainty is applied separately to each MC process contributing to the estimate, i.e.

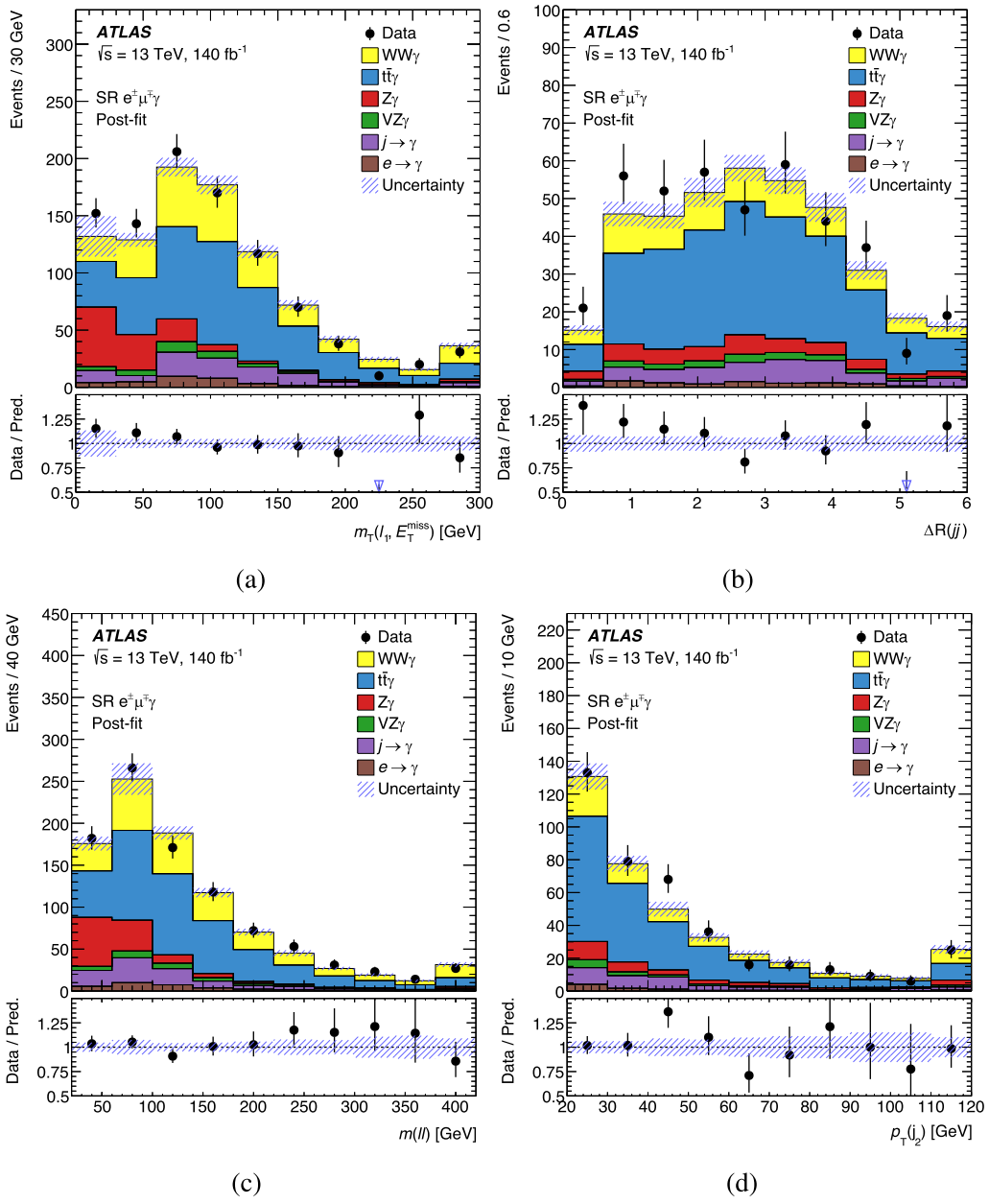

Fig. 2. Comparison between data and prediction ("Pred.") for the four most discriminating BDT input variables after the fit to data ("Post-Fit") under the signal-plus-background hypothesis, shown in the SR. The variables displayed are (a) $m_{\mathrm{T}}(\ell_1, E_{\mathrm{T}}^{\mathrm{miss}})$, (b) $\Delta R(jj)$, (c) $m(\ell\ell)$, and (d) $p_{\mathrm{T}}(j_2)$. The uncertainty band includes both the statistical and systematic uncertainties as obtained from the fit. The rightmost bin includes overflow events. The lower panels show the ratio of data to prediction. Open markers indicate data points lying outside the vertical range of the plot.

$t\bar{t}$, Z + jets, and $VV\gamma$ as detailed in Section 5, and contributes approximately 2.5 % to the measurement uncertainty.

An additional uncertainty associated with the $j \to \gamma$ misidentification is applied separately to processes involving light-flavour jets, such as Z + jets and VV, and to those involving heavy-flavour jets, such as $t\bar{t}$ and tW. The total contribution from $j \to \gamma$ misidentification to the overall uncertainty is approximately 4.5 %.

A systematic uncertainty is assigned to the $e \to \gamma$ background to account for the limited numbers of data and MC events in the $e\gamma$ and $e^{\pm}e^{\mp}$ regions. An additional uncertainty, estimated by using the alternative non-resonant background model described in Section 5, affects the measurement uncertainty by less than 1 %. In total, the data-driven background estimate contributes a 5.4 % uncertainty to the measurement.

Background rate uncertainty: For the $VZ\gamma$ process, a 20 % normalisation uncertainty is applied, motivated by the $WZ\gamma$ measurement [13]. This accounts for uncertainties from the PDFs, renormalisation and factorisation scale variations, and other possible missing higher-order QCD corrections.

8. Results

To extract the $WW\gamma$ signal strength, a simultaneous binned maximum-likelihood fit is performed on the BDT output distributions in the $WW\gamma$ SR and the $t\bar{t}\gamma$, $Z\gamma$ and $e \to \gamma$ CRs. The fit is implemented using the `TRExFitter` framework [74], which builds upon `HistFactory` [75] and `RooFit` [76].

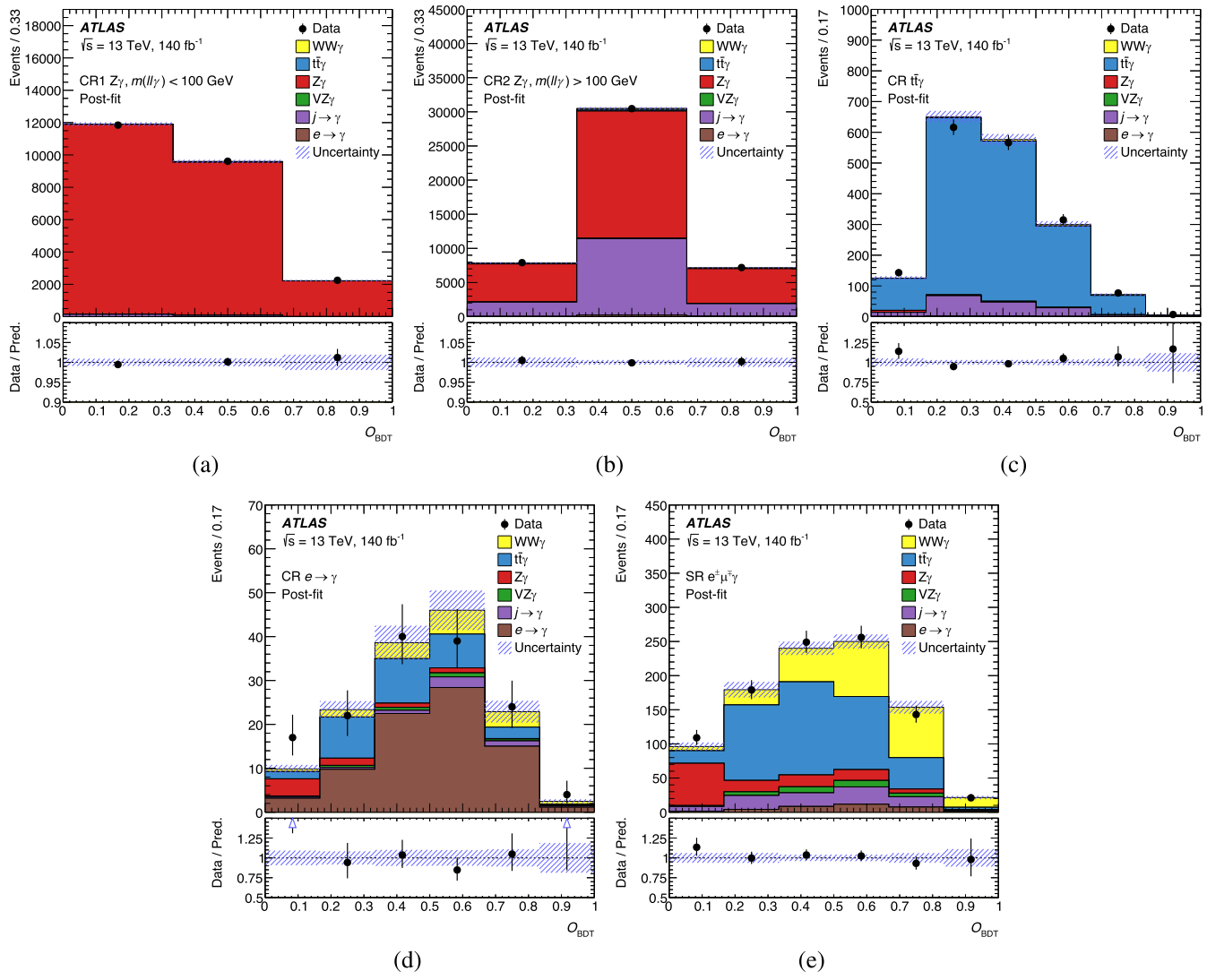

Fig. 3. Comparison between data and the post-fit prediction ("Pred."), under the signal-plus-background hypothesis, from the distributions of the boosted decision tree output (O_{BDT}) in the (a) $Z\gamma$ CR1, (b) $Z\gamma$ CR2, (c) $t\bar{t}\gamma$ CR, (d) $e \to \gamma$ CR, and (e) $e^{\pm}\mu^{\mp}\nu\bar{\nu}\gamma$ SR. The uncertainty band includes both the statistical and systematic uncertainties as obtained from the fit.The lower panels show the ratio of data to prediction. The open markers indicate data points lying outside the vertical range of the lower panel in (d).

The BDT trained in the SR is evaluated on the events selected in the corresponding CRs. Five unconstrained fit parameters corresponding to the $WW\gamma$, $t\bar{t}\gamma$, $Z\gamma$, $j \to \gamma$, and $e \to \gamma$ normalisations are included. Nuisance parameters are included in the fit to account for each systematic uncertainty described in Section 7.

Fig. 3 compares the BDT output distribution for the data with those for the post-fit signal and backgrounds. The numbers of fitted signal and background events are compared with the data in Table 3. The normalisation of the $WW\gamma$ signal is $1.03^{+0.22}_{-0.21}$, in good agreement with the SM prediction, and includes the uncertainty from the predicted fiducial cross-section. The measured normalisation parameters for the backgrounds are also consistent with the SM predictions within uncertainties.

To obtain the $WW\gamma$ fiducial production cross-section, a fiducial volume is defined at particle level to closely match the selection criteria of the SR. Events are selected if they contain at least one photon, and one muon and one electron with opposite electric charges. Electrons and muons, excluding those originating from τ-lepton decays, are "dressed" by adding all nearby photons within a cone of size $\Delta R = 0.1$. The dressed leptons are then required to have $p_{\text{T}} > 20\,\text{GeV}$ and $|\eta| < 2.5$. Final-state photons must be prompt, with $p_{\text{T}} > 20\,\text{GeV}$ and $|\eta| < 2.37$, and satisfy a particle-level isolation requirement: the scalar sum of the transverse energy (E_{T}) of all stable particles, excluding neutrinos, within $\Delta R = 0.2$ of the photon must be less than 7 % of the photon E_{T}, i.e. $E_{\text{T}}^{\text{iso}}/E_{\text{T}}^{\gamma} < 0.07$. Photons within $\Delta R = 0.4$ of a selected muon or electron are discarded.

Table 3
Predicted and observed event yields in the signal region (SR) and control regions (CR). The signal and background predictions are shown after the fit to data. The uncertainties include the statistical and systematic uncertainties of the yields, and also the correlations among nuisance parameters, as well as correlations across signal and background processes because of shared systematic effects.

	SR $e^{\pm}\mu^{\mp}\nu\bar{\nu}\gamma$	CR $t\bar{t}\gamma$	CR1 $Z\gamma$	CR2 $Z\gamma$	CR $e \to \gamma$
$WW\gamma$	250 ± 40	17.7 ± 3.4	42 ± 6	290 ± 40	15.5 ± 2.4
$VZ\gamma$	31 ± 6	3.7 ± 0.8	35 ± 7	123 ± 25	2.7 ± 0.5
$Z\gamma$	119 ± 7	10.7 ± 1.2	23,390 ± 180	29,300 ± 800	7.7 ± 0.7
$t\bar{t}\gamma$	422 ± 34	1530 ± 90	38.9 ± 3.3	418 ± 33	31.8 ± 2.9
$j \to \gamma$	89 ± 34	160 ± 90	220 ± 80	15,100 ± 800	5.5 ± 1.6
$e \to \gamma$	34 ± 5	8.1 ± 1.3	4.4 ± 0.8	330 ± 50	80 ± 13
Total	941 ± 29	1730 ± 40	23,730 ± 160	45,560 ± 230	143 ± 12
Data	957	1724	23707	45570	146

Table 4
The impact of systematic uncertainties on the measured $WW\gamma$ fiducial cross-section, decomposed into their major categories. For each category, the contribution is obtained by summing in quadrature the impacts of its nuisance parameters. The total systematic uncertainty is calculated similarly by combining all nuisance parameter impacts in quadrature. The statistical uncertainty is calculated as the square root of the difference of the squares of the total uncertainty and the total systematic uncertainty.

Uncertainty source	$\Delta\sigma/\sigma$ [%]
Non-prompt-photon background modelling	5.4
Jet energy scale and resolution	4.1
Jet flavour tagging	3.0
MC statistics	2.9
Signal modelling	2.8
Pile-up modelling	2.5
Lepton reconstruction and calibration	2.3
Prompt-photon background modelling	2.1
Photon reconstruction and calibration	2.0
$E_{\mathrm{T}}^{\mathrm{miss}}$ reconstruction and calibration	1.1
Luminosity	0.9
Total systematic uncertainty	9.6
Statistical uncertainty	12
Total uncertainty	16

Additionally, at least one muon or electron must have $p_{\mathrm{T}} > 27$ GeV. Finally, events with particle-level jets containing b-hadrons are removed, where jets are required to have $p_{\mathrm{T}} > 20$ GeV and $|\eta| < 4.5$. This requirement rejects about 1 % of events when evaluated on the $WW\gamma$ samples. The fiducial cross-section includes non-resonant and off-shell $WW\gamma$ contributions, which amount to <1 % of the predicted fiducial cross-section. Using the signal MC sample described in Section 3, the predicted fiducial cross-section is $\sigma_{\mathrm{fid}} = 6.1^{+1.0}_{-0.7}$ fb. Renormalisation and factorisation scale uncertainties contribute $^{+17}_{-11}$%, evaluated from the envelope of seven-point scale variations where the scales are raised or lowered by a factor of two, excluding combinations where one scale is raised and the other lowered. The PDF uncertainty contributes 0.13 %, evaluated using the RMS of the 100 replicas in the NNPDF3.0NNLO PDF set. An uncertainty of 0.8 % arises from varying the strong coupling constant α_{s} by ±0.001 via the PDFs named NNPDF30_nnlo_as_119 and NNPDF30_nnlo_as_117.

The measured $WW\gamma$ fiducial production cross-section is $6.2 \pm 0.8\,(\mathrm{stat.}) \pm 0.6\,(\mathrm{sys.})$ fb $= 6.2 \pm 1.0$ fb, which corresponds to a total uncertainty of 16 %. The total systematic uncertainty is calculated by combining all nuisance parameter impacts in quadrature. The impact of a nuisance parameter on the signal strength is quantified by the corresponding off-diagonal element of the post-fit covariance matrix [77]. In the case of nuisance parameters representing the MC statistical uncertainty in each bin, their impacts are evaluated by dividing their post-fit off-diagonal elements by their corresponding pre-fit uncertainties. The uncertainty of the measured cross-section is dominated by a statistical uncertainty of 12 %, calculated as the square root of the difference of the squares of the total uncertainty and the total systematic uncertainty. The impact of systematic uncertainties on the measured signal strength is grouped into categories and summarised in Table 4.

The probability of the background processes alone producing a signal-like excess at least as large as that seen in data is derived using the profile-likelihood-ratio test statistic in the asymptotic approximation [78]. The significance of the observed signal is 5.9σ, compared to an expected significance of 6.0σ.

9. EFT interpretation

Potential deviations from the SM predictions, such as in cross-section values or kinematic distributions, are modelled using an EFT framework, which extends the SM Lagrangian to include higher-dimensional operators that parameterise new physics at energy scales beyond the SM. In this analysis, the Eboli parameterisation [17] is used, focusing exclusively on dimension-8 operators acting on quartic gauge-boson couplings. Dimension-6 operators relevant to triple gauge-boson couplings have already been tightly constrained by ATLAS [79–82] and CMS [83–89] analyses of diboson processes. Since the $WW\gamma$ channel offers substantially weaker sensitivity compared with existing diboson measurements, the contributions of dimension-6 operators are not investigated in this analysis.

The $WW\gamma\gamma$ and $WWZ\gamma$ vertices are sensitive to 13 dimension-8 operators defined in Ref. [17], called $\mathcal{O}_{\mathrm{M0}}$, $\mathcal{O}_{\mathrm{M1}}$, $\mathcal{O}_{\mathrm{M2}}$, $\mathcal{O}_{\mathrm{M3}}$, $\mathcal{O}_{\mathrm{M4}}$, $\mathcal{O}_{\mathrm{M5}}$, $\mathcal{O}_{\mathrm{M7}}$, $\mathcal{O}_{\mathrm{T0}}$, $\mathcal{O}_{\mathrm{T1}}$, $\mathcal{O}_{\mathrm{T2}}$, $\mathcal{O}_{\mathrm{T5}}$, $\mathcal{O}_{\mathrm{T6}}$, and $\mathcal{O}_{\mathrm{T7}}$. Each operator is associated with a Wilson coefficient (f_i), which parametrises the strength of the corresponding higher-dimensional interaction. These operators correspond to two classes of mixed-scalar operators, consisting of two covariant derivatives of the Higgs field and two field-strength tensors, and tensor-type operators, consisting of four field-strength tensors.

The effects of higher-dimensional beyond-the-SM (BSM) operators are more pronounced at high photon p_{T}. To enhance the sensitivity of the analysis to such effects, the SR used for the SM $WW\gamma$ measurement is split into two regions: a one-bin high-$p_{\mathrm{T}}(\gamma)$ signal region with $p_{\mathrm{T}}(\gamma) > 500$ GeV, and a CR with $p_{\mathrm{T}}(\gamma) < 500$ GeV, where the BDT distribution is used. The threshold at 500 GeV is chosen to optimise the expected signal-to-background ratio for BSM contributions, resulting in negligible BSM sensitivity in all CRs including the low-$p_{\mathrm{T}}(\gamma)$ CR, while maximising it in the high-$p_{\mathrm{T}}(\gamma)$ bin. The photon p_{T} distribution used to define these regions is provided in the Appendix A. The expected yield, including the SM $WW\gamma$ contribution, in the high-$p_{\mathrm{T}}(\gamma)$ region is 2.24 ± 0.31, whereas one event is observed in data.

A simultaneous binned maximum-likelihood fit is performed for each dimension-8 operator independently, neglecting possible interference between operators, and using the high-$p_{\mathrm{T}}(\gamma)$ EFT region together with the CRs, following the same set-up as in the $WW\gamma$ measurement. The SM background normalisations, including that of SM $WW\gamma$, are treated as free parameters in the likelihood fit. Additional unconstrained fit parameter is defined such that f_i^2 is the normalisation factor of events arising from BSM contributions, while events arising from interference between SM and BSM amplitudes are scaled by f_i. Additional modelling uncertainties for the BSM contributions are taken into account, including those from the PDF, μ_{r} and μ_{f}. A one-dimensional 95 % confidence interval (CI) for each Wilson coefficient is derived from the profile-likelihood curves using the criterion $-2 \cdot \Delta \ln \mathcal{L} = 3.84$, as prescribed by Wilks' theorem [90].

The expected and observed 95 % CIs for the Wilson coefficients are presented in Table 5. The sensitivity is statistically limited: including all systematic uncertainties changes the expected interval widths by less than 1 %. These limits are comparable to limits obtained from vector-boson scattering measurements and $Z(\nu\nu)\gamma$ [65], $W\gamma jj$ [91] and VVZ productions [15].

Limits on the dimension-8 Wilson coefficients are also evaluated as functions of a cut-off scale, $\sqrt{\hat{s}}$, using the clipping technique [92]. For events with $\sqrt{\hat{s}}$ greater than the cut-off, the EFT contribution is set to zero. The unitarity bounds for aQGC operators, as derived in Ref. [93], are formulated for 2-to-2 scattering processes in proton-proton collisions. To extend these bounds to $WW\gamma$ production, $\sqrt{\hat{s}}$ is set to the maximum of the three diboson invariant mass combinations, $\max(m_{V_iV_j})$.

The most stringent limit respecting unitarity is found at the intersection of the calculated limits with the unitarity bounds. Among the 13 coefficients investigated, four coefficients exhibit a range of values that respect unitarity: $[-9.5, 9.5]$ TeV^{-4} at $\sqrt{\hat{s}} = 1.9$ TeV for $f_{\mathrm{M3}}/\Lambda^4$, $[-10, 10]$ TeV^{-4} at 2.0 TeV for $f_{\mathrm{M5}}/\Lambda^4$, $[-4, 4]$ TeV^{-4} at 1.5 TeV for $f_{\mathrm{T6}}/\Lambda^4$, and $[-10.5, 10.5]$ TeV^{-4} at 1.5 TeV for $f_{\mathrm{T7}}/\Lambda^4$. Fig. 4 shows the 95 % CI for the $f_{\mathrm{M3}}/\Lambda^4$ Wilson coefficient as a function of the cut-off scale applied to restore unitarity.

Table 5
Expected and observed non-unitarised 95 % CIs for the 13 dimension-8 Wilson coefficients The expected CIs are derived from an Asimov dataset constructed in two steps: first, the control regions, including the SM $WW\gamma$ CR, are fitted assuming no EFT contribution to extract the background normalisations; second, a signal-plus-background fit is performed using an Asimov dataset built from these fitted normalisations.

EFT operator	Expected 95 % CI [TeV^{-4}]	Observed 95 % CI [TeV^{-4}]
f_{M0}/Λ^4	$[-8, 8]$	$[-6, 6]$
f_{M1}/Λ^4	$[-13, 13]$	$[-10, 10]$
f_{M2}/Λ^4	$[-3.1, 3.1]$	$[-2.5, 2.5]$
f_{M3}/Λ^4	$[-5, 5]$	$[-4, 4]$
f_{M4}/Λ^4	$[-8, 8]$	$[-6, 6]$
f_{M5}/Λ^4	$[-6, 6]$	$[-5, 5]$
f_{M7}/Λ^4	$[-26, 26]$	$[-21, 21]$
f_{T0}/Λ^4	$[-1.4, 1.4]$	$[-1.1, 1.1]$
f_{T1}/Λ^4	$[-1.7, 1.7]$	$[-1.4, 1.3]$
f_{T2}/Λ^4	$[-4, 4]$	$[-3.1, 3.0]$
f_{T5}/Λ^4	$[-1.1, 1.1]$	$[-0.9, 0.9]$
f_{T6}/Λ^4	$[-1.3, 1.3]$	$[-1.1, 1.1]$
f_{T7}/Λ^4	$[-3.0, 3.0]$	$[-2.4, 2.4]$

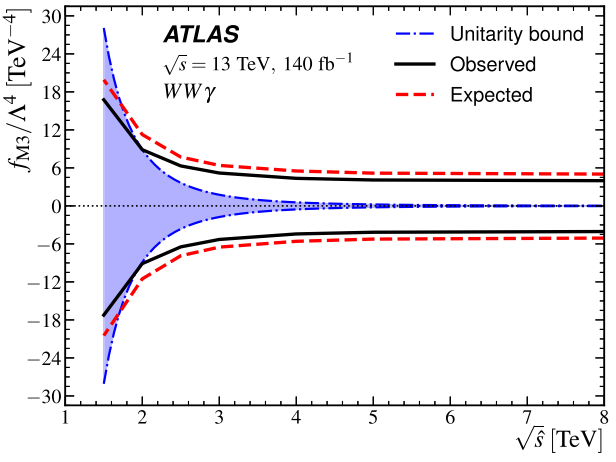

Fig. 4. The 95 % confidence interval of the f_{M3}/Λ^4 Wilson coefficient as a function of the energy threshold used in the clipping method to restore unitarity. The blue dash-dotted lines indicate the unitarity bound. The black solid lines show the observed upper and lower limits, while the red dashed lines show the expected upper and lower limits.

10. Conclusion

The production of $WW\gamma$ events is observed with a significance of 5.9σ, compared to an expected significance of 6.0σ, using the $e^{\pm}\mu^{\mp}\nu\bar{\nu}\gamma$ final state and $140\,\text{fb}^{-1}$ of data from 13 TeV proton–proton collisions recorded by the ATLAS detector at the LHC between 2015 and 2018.

The measured fiducial cross-section in the $e^{\pm}\mu^{\mp}\nu\bar{\nu}\gamma$ final state is $6.2 \pm 0.8\,(\text{stat.}) \pm 0.6\,(\text{sys.})\,\text{fb} = 6.2 \pm 1.0\,\text{fb}$, corresponding to a total uncertainty of 16 %. This measurement is in good agreement with the SM prediction of $6.1^{+1.0}_{-0.7}\,\text{fb}$, calculated at NLO in QCD for $WW\gamma$ + 0-jet events and at LO for events with one or two additional jets.

In addition, constraints at the 95 % confidence level are set on 13 dimension-8 EFT Wilson coefficients within the effective field theory framework. These constitute the first limits from the $WW\gamma$ channel, probing aQGC at high photon transverse momentum. They are complementary to existing multiboson results and provide valuable input to the global EFT interpretation of QGC.

Declaration of interests

The authors declare that they have no known competing financial interests or personal relationships that could have appeared to influence the work reported in this paper.

Acknowledgements

We thank CERN for the very successful operation of the LHC and its injectors, as well as the support staff at CERN and at our institutions worldwide without whom ATLAS could not be operated efficiently.

The crucial computing support from all WLCG partners is acknowledged gratefully, in particular from CERN, the ATLAS Tier-1 facilities at TRIUMF/SFU (Canada), NDGF (Denmark, Norway, Sweden), CC-IN2P3 (France), KIT/GridKA (Germany), INFN-CNAF (Italy), NL-T1 (Netherlands), PIC (Spain), RAL (UK) and BNL (USA), the Tier-2 facilities worldwide and large non-WLCG resource providers. Major contributors of computing resources are listed in Ref. [94].

We gratefully acknowledge the support of ANPCyT, Argentina; YerPhI, Armenia; ARC, Australia; BMWFW and FWF, Austria; ANAS, Azerbaijan; CNPq and FAPESP, Brazil; NSERC, NRC and CFI, Canada; CERN; ANID, Chile; CAS, MOST and NSFC, China; Minciencias, Colombia; MEYS CR, Czech Republic; DNRF and DNSRC, Denmark; IN2P3-CNRS and CEA-DRF/IRFU, France; SRNSFG, Georgia; BMFTR, HGF and MPG, Germany; GSRI, Greece; RGC and Hong Kong SAR, China; ICHEP and Academy of Sciences and Humanities, Israel; INFN, Italy; MEXT and JSPS, Japan; CNRST, Morocco; NWO, Netherlands; RCN, Norway; MNiSW, Poland; FCT, Portugal; MNE/IFA, Romania; MSTDI, Serbia; MSSR, Slovakia; ARIS and MVZI, Slovenia; DSI/NRF, South Africa; MICIU/AEI, Spain; SRC and Wallenberg Foundation, Sweden; SERI, SNSF and Cantons of Bern and Geneva, Switzerland; NSTC, Taipei; TENMAK, Türkiye; STFC/UKRI, United Kingdom; DOE and NSF, United States of America.

Individual groups and members have received support from BCKDF, CANARIE, CRC and DRAC, Canada; CERN-CZ, FORTE and PRIMUS, Czech Republic; COST, ERC, ERDF, Horizon 2020, ICSC-NextGenerationEU and Marie Skłodowska-Curie Actions, European Union; Investissements d'Avenir Labex, Investissements d'Avenir Idex and ANR, France; DFG and AvH Foundation, Germany; Herakleitos, Thales and Aristeia programmes co-financed by EU-ESF and the Greek NSRF, Greece; BSF-NSF and MINERVA, Israel; NCN and NAWA, Poland; La Caixa Banking Foundation, CERCA Programme Generalitat de Catalunya and PROMETEO and GenT Programmes Generalitat Valenciana, Spain; Göran Gustafssons Stiftelse, Sweden; The Royal Society and Leverhulme Trust, United Kingdom.

In addition, individual members wish to acknowledge support from CERN: European Organization for Nuclear Research (CERN DOCT); Chile: Agencia Nacional de Investigación y Desarrollo (FONDECYT 1230812, FONDECYT 1240864, Fondecyt 3240661, Fondecyt Regular 1240721); China: Chinese Ministry of Science and Technology (MOST-2023YFA1605700, MOST-2023YFA1609300), National Natural Science Foundation of China (NSFC - 12175119, NSFC 12275265); Czech Republic: Czech Science Foundation (GACR - 24-11373S), Ministry of Education Youth and Sports (ERC-CZ-LL2327, FORTE CZ.02.01.01/00/22_008/0004632), PRIMUS Research Programme (PRIMUS/21/SCI/017); EU: H2020 European Research Council (ERC - 101002463); European Union: European Research Council (BARD No. 101116429, ERC - 948254, ERC 101089007), European Regional Development Fund (SMASH COFUND 101081355, SLO ERDF), European Union, Future Artificial Intelligence Research (FAIR-NextGenerationEU PE00000013), Italian Center for High Performance Computing, Big Data and Quantum Computing (ICSC, NextGenerationEU); France: Agence Nationale de la Recherche (ANR-21-CE31-0022, ANR-22-EDIR-0002, ANR-24-CE31-0504-01); Germany: Baden-Württemberg Stiftung (BW Stiftung-Postdoc Eliteprogramme), Deutsche Forschungsgemeinschaft (DFG - 469666862, DFG - CR 312/5-2); China: Research

Grants Council (GRF); Italy: Istituto Nazionale di Fisica Nucleare (ICSC, NextGenerationEU), Ministero dell'Università e della Ricerca (NextGenEU 153D23001490006 M4C2.1.1, NextGenEU I53D23000820006 M4C2.1.1, NextGenEU I53D23001490006 M4C2.1.1, SOE2024_0000023); Japan: Japan Society for the Promotion of Science (JSPS KAKENHI JP22H01227, JSPS KAKENHI JP22H04944, JSPS KAKENHI JP22KK0227, JSPS KAKENHI JP24K23939, JSPS KAKENHI JP24KK0251, JSPS KAKENHI JP25H00650, JSPS KAKENHI JP25H01291, JSPS KAKENHI JP25K01023); Norway: Research Council of Norway (RCN-314472); Poland: Ministry of Science and Higher Education (IDUB AGH, POB8, D4 no 9722), Polish National Science Centre (NCN 2021/42/E/ST2/00350, NCN OPUS 2023/51/B/ST2/02507, NCN UMO-2019/34/E/ST2/00393, UMO-2022/47/O/ST2/00148, UMO-2023/49/B/ST2/04085, UMO-2023/51/B/ST2/00920, UMO-2024/53/N/ST2/00869); Portugal: Foundation for Science and Technology (FCT); Spain: Ministry of Science and Innovation (MCIN & NextGenEU PCI2022-135018-2, MICIN & FEDER PID2021-125273NB, RYC2019-028510-I, RYC2020-030254-I, RYC2021-031273-I, RYC2022-038164-I), Ministerio de Ciencia, Innovación y Universidades/Agencia Estatal de Investigación (PID2022-142604OB-C22); Sweden: Carl Trygger Foundation (Carl Trygger Foundation CTS 22:2312), Swedish Research Council (Swedish Research Council 2023-04654, VR 2021-03651, VR 2022-03845, VR 2022-04683, VR 2023-03403, VR 2024-05451), Knut and Alice Wallenberg Foundation (KAW 2018.0458, KAW 2022.0358, KAW 2023.0366); Switzerland: Swiss National Science Foundation (SNSF - PCEFP2_194658); United Kingdom: Royal Society (NIF-R1-231091); United States of America: U.S. Department of Energy (ECA DE-AC02-76SF00515), Neubauer Family Foundation.

Appendix A.

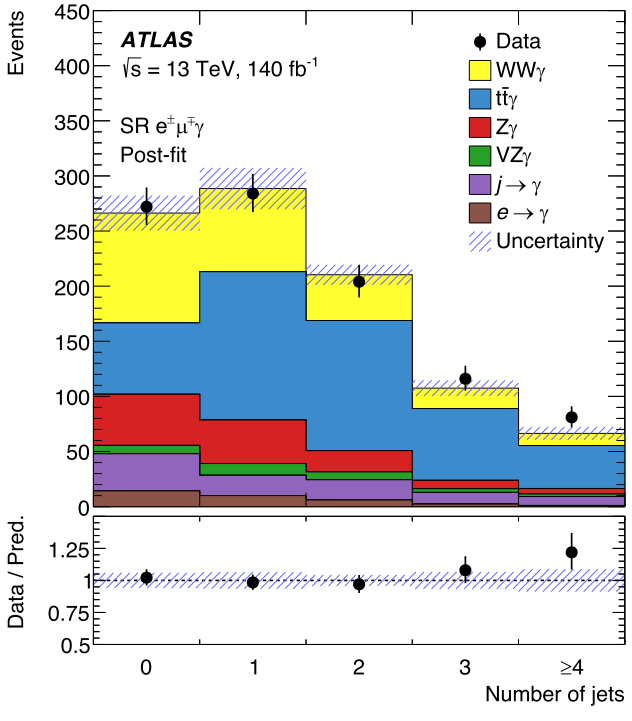

Fig. A.5. Comparison between data and prediction ("Pred.") for the jet multiplicity distribution after the fit to data ("Post-Fit") under the signal-plus-background hypothesis, shown in the SR. The uncertainty band includes both statistical and systematic uncertainties as obtained from the fit. The rightmost bin includes overflow events.

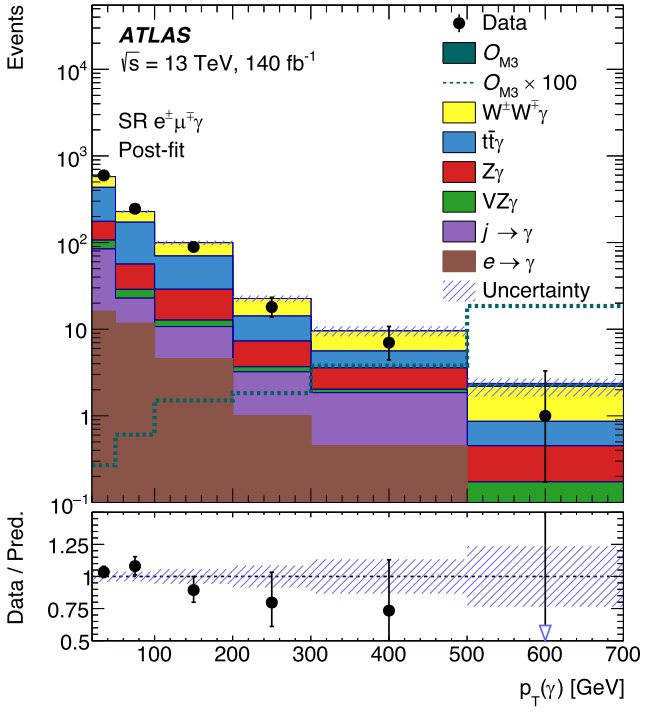

Fig. A.6. Comparison between data and prediction ("Pred.") for the photon p_{T} distribution after the fit to data ("Post-fit") under the signal-plus-background hypothesis including $\mathcal{O}_{\mathrm{M3}}$ operator, shown in the $WW\gamma$ SR. The uncertainty band includes both statistical and systematic uncertainties as obtained from the fit.The rightmost bin includes overflow events.The contribution of the Wilson coefficient $f_{\mathrm{M3}}/\Lambda^4$ is shown as shaded teal area and is normalised to the prediction for a coefficient value of 1 TeV^{-4}. The dashed teal line corresponds to the same prediction multiplied by a factor of 100. The EFT sensitivity is enhanced when the photon p_{T} is above 500 GeV.

ATLAS Collaboration

G. Aad[154], E. Aakvaag[18], B. Abbott[176], S. Abdelhameed[171], K. Abeling[84], N.J. Abicht[78], S.H. Abidi[43], M. Aboelela[73], A. Aboulhorma[62], H. Abramowicz[226], Y. Abulaiti[173], B.S. Acharya[XIII,102,103], A. Ackermann[93], C. Adam Bourdarios[5], L. Adamczyk[136], S.V. Addepalli[216], M. J. Addison[153], J. Adelman[170], A. Adiguzel[26], T. Adye[196], A.A. Affolder[198], Y. Afik[67], M.N. Agaras[14], A. Aggarwal[152], C. Agheorghiesei[36], F. Ahmadov[XXX,66], S. Ahuja[147], S. Ahuja[239], X. Ai[209], G. Aielli[117,118], A. Aikot[239], M. Ait Tamlihat[62], B. Aitbenchikh[58], M. Akbiyik[152], T.P.A. Åkesson[150], A.V. Akimov[218], D. Akiyama[244], N.N. Akolkar[31], S. Aktas[242], G.L. Alberghi[30], J. Albert[241], U. Alberti[22], P. Albicocco[82], G.L. Albouy[90], S. Alderweireldt[81], Z.L. Alegria[177], M. Aleksa[64], I.N. Aleksandrov[66], C. Alexa[35], T. Alexopoulos[11], F. Alfonsi[30], M. Algren[85], M. Alhroob[243], B. Ali[194], H. M. J. Ali[XXIII,143], S. Ali[45], S.W. Alibocus[144], M. Aliev[49], G. Alimonti[107], W. Alkakhi[84], C. Allaire[99], B.M.M. Allbrooke[219], D. R. Allen[177], J. S. Allen[153], J.F. Allen[81], P.P. Allport[23], A. Aloisio[109,110], F. Alonso[142], C. Alpigiani[207], Z.M.K. Alsolami[143], A. Alvarez Fernandez[152], M. Alves Cardoso[85], M.G. Alviggi[109,110], M. Aly[153], Y. Amaral Coutinho[128], A. Ambler[156], C. Amelung[64], M. Amerl[153], C.G. Ames[161], T. Amezza[183], D. Amidei[158], B. Amini[83], K. Amirie[230], A. Amirkhanov[66], S.P. Amor Dos Santos[186], K.R. Amos[239], D. Amperiadou[227], S. An[132], C. Anastopoulos[212], T. Andeen[12], J.K. Anders[144], A. C. Anderson[89], A. Andreazza[107,108], S. Angelidakis[10], A. Angerami[69], A.V. Anisenkov[66], A. Annovi[113], C. Antel[64], E. Antipov[218], M. Antonelli[82], F. Anulli[115], M. Aoki[132],

T. Aoki[228], M.A. Aparo[219], L. Aperio Bella[77], M. Apicella[44], C. Appelt[226], A. Apyan[33], M. Arampatzi[11], S. J. Arbiol Val[138], C. Arcangeletti[82], A.T.H. Arce[80], J-F. Arguin[160], S. Argyropoulos[227], J.-H. Arling[77], O. Arnaez[5], H. Arnold[218], G. Artoni[115,116], H. Asada[163], K. Asai[174], S. Asatryan[249], N.A. Asbah[64], R. A. Ashby Pickering[243], A. M. Aslam[147], K. Assamagan[43], R. Astalos[41], K. S. V. Astrand[150], S. Atashi[235], R.J. Atkin[47], H. Atmani[63], P.A. Atmasiddha[184], K. Augsten[194], A.D. Auriol[68], V.A. Austrup[153], A.S. Avad[146], G. Avolio[64], K. Axiotis[85], A. Azzam[14], D. Babal[42], H. Bachacou[197], K. Bachas[XVII,227], A. Bachiu[57], E. Bachmann[79], M. J. Backes[93], A. Badea[67], T.M. Baer[158], P. Bagnaia[115,116], M. Bahmani[21], D. Bahner[83], K. Bai[179], J.T. Baines[196], L. Baines[146], O.K. Baker[248], E. Bakos[17], D. Bakshi Gupta[9], L.E. Balabram Filho[128], V. Balakrishnan[176], R. Balasubramanian[5], E.M. Baldin[65], P. Balek[136], E. Ballabene[30,29], F. Balli[197], L.M. Baltes[93], W.K. Balunas[46], J. Balz[152], I. Bamwidhi[172], E. Banas[138], M. Bandieramonte[185], A. Bandyopadhyay[31], S. Bansal[31], L. Barak[226], M. Barakat[77], E.L. Barberio[157], D. Barberis[20], M. Barbero[154], M. Z. Barel[169], T. Barillari[162], M-S. Barisits[64], T. Barklow[216], P. Baron[195], D.A. Baron Moreno[153], A. Baroncelli[92], A.J. Barr[182], J.D. Barr[148], F. Barreiro[151], J. Barreiro Guimarães da Costa[15], M.G. Barros Teixeira[186], S. Barsov[65], F. Bartels[93], R. Bartoldus[216], A.E. Barton[143], P. Bartos[41], M. Baselga[78], S. Bashiri[138], A. Bassalat[II,99], M.J. Basso[231], S. Bataju[73], R. Bate[240], R.L. Bates[89], S. Batlamous[151], M. Battaglia[198], D. Battulga[21], M. Bauce[115,116], M. Bauer[123], P. Bauer[31], L. T. Bayer[77], L.T. Bazzano Hurrell[44], J.B. Beacham[162], T. Beau[183], J.Y. Beaucamp[142], P.H. Beauchemin[234], P. Bechtle[31], H.P. Beck[XVI,22], K. Becker[243], A.J. Beddall[126], V.A. Bednyakov[66], C.P. Bee[218], L.J. Beemster[17], M. Begalli[130], M. Begel[43], J.K. Behr[77], J.F. Beirer[64], F. Beisiegel[31], M. Belfkir[172], G. Bella[226], L. Bellagamba[30], A. Bellerive[57], C.D. Bellgraph[101], P. Bellos[23], K. Beloborodov[65], I. Benaoumeur[23], D. Benchekroun[58], F. Bendebba[58], Y. Benhammou[226], K.C. Benkendorfer[91], L. Beresford[77], M. Beretta[82], E. Bergeaas Kuutmann[237], N. Berger[5], B. Bergmann[194], J. Beringer[19], G. Bernardi[6], C. Bernius[216], F.U. Bernlochner[31], A. Berrocal Guardia[14], T. Berry[147], P. Berta[195], A. Berthold[79], A. Berti[186], R. Bertrand[154], S. Bethke[162], A. Betti[115,116], A.J. Bevan[146], L. Bezio[85], N.K. Bhalla[83], S. Bharthuar[162], S. Bhatta[218], P. Bhattarai[216], Z.M. Bhatti[173], K. D. Bhide[83], V.S. Bhopatkar[177], R.M. Bianchi[185], G. Bianco[30,29], O. Biebel[161], M. Biglietti[119], C. S. Billingsley[73], Y. Bimgdi[63], M. Bindi[84], A. Bingham[247], A. Bingul[25], C. Bini[115,116], G.A. Bird[46], M. Birman[245], M. Biros[195], S. Biryukov[219], T. Bisanz[78], E. Bisceglie[30,29], J.P. Biswal[196], D. Biswas[214], I. Bloch[77], A. Blue[89], U. Blumenschein[146], V.S. Bobrovnikov[66], L. Boccardo[87,86], M. Boehler[83], B. Boehm[242], D. Bogavac[14], A.G. Bogdanchikov[65], L. S. Boggia[183], V. Boisvert[147], P. Bokan[64], T. Bold[136], M. Bomben[6], M. Bona[146], M. Boonekamp[197], A.G. Borbély[89], I.S. Bordulev[65], G. Borissov[143], D. Bortoletto[182], D. Boscherini[30], M. Bosman[14], K. Bouaouda[58], N. Bouchhar[239], L. Boudet[5], J. Boudreau[185], E.V. Bouhova-Thacker[143], D. Boumediene[68], R. Bouquet[87,86], A. Boveia[175], J. Boyd[64], D. Boye[43], I.R. Boyko[66], L. Bozianu[85], J. Bracinik[23], N. Brahimi[5], G. Brandt[247], O. Brandt[46], B. Brau[155], J.E. Brau[179], R. Brener[245], L. Brenner[169], R. Brenner[237], S. Bressler[245], G. Brianti[121,122], D. Britton[89], D. Britzger[162], I. Brock[31], R. Brock[159], G. Brooijmans[69], A.J. Brooks[101], E. M. Brooks[232], E. Brost[43], L.M. Brown[241,231], L.E. Bruce[91], T.L. Bruckler[182], P.A. Bruckman de Renstrom[138], B. Brüers[77], A. Bruni[30], G. Bruni[30], D. Brunner[75,76], M. Bruschi[30], N. Bruscino[115,116], T. Buanes[18], Q. Buat[207], D. Buchin[162], A.G. Buckley[89], O. Bulekov[126], B.A. Bullard[216], S. Burdin[144], C.D. Burgard[78], A.M. Burger[141], B. Burghgrave[9], O. Burlayenko[83], J. Burleson[238], J.C. Burzynski[215], E.L. Busch[69], V. Büscher[152], P.J. Bussey[89], O. But[31], J.M. Butler[32], C.M. Buttar[89], J.M. Butterworth[148], W. Buttinger[196], C.J. Buxo Vazquez[159], A.R. Buzykaev[66], S. Cabrera Urbán[239], L. Cadamuro[99], H. Cai[64], Y. Cai[30,166,29], Y. Cai[164], V.M.M. Cairo[64], O. Cakir[3], N. Calace[64], P. Calafiura[19], G. Calderini[183], P. Calfayan[57], L. Calic[150], G. Callea[89], L.P. Caloba[128], D. Calvet[68], S. Calvet[68], R. Camacho Toro[183], S. Camarda[64], D. Camarero Munoz[33], P. Camarri[117,118], C. Camincher[241], M. Campanelli[148], A. Camplani[70], V. Canale[109,110], A.C. Canbay[3], E. Canonero[147], J. Cantero[239], Y. Cao[238], F. Capocasa[33], M. Capua[72,71], A. Carbone[107,108], R. Cardarelli[117], J.C.J. Cardenas[9], M. P. Cardiff[33], G. Carducci[72,71], T. Carli[64], G. Carlino[109], J.I. Carlotto[14], B.T. Carlson[XVIII,185], E.M. Carlson[241], J. Carmignani[144], L. Carminati[107,108], A. Carnelli[5], M. Carnesale[64], S. Caron[168], E. Carquin[205], I.B. Carr[157], S. Carrá[111,112], G. Carratta[30,29], C. Carrion Martinez[239], A.M. Carroll[179], M.P. Casado[VIII,14], P. Casolaro[109,110], M. Caspar[77], W.R. Castiglioni[67], F.L. Castillo[5], L. Castillo Garcia[14], V. Castillo Gimenez[239], N.F. Castro[186,190], A. Catinaccio[64], J.R. Catmore[181], T. Cavaliere[5], V. Cavaliere[43], L.J. Caviedes Betancourt[28], E. Celebi[126], S. Cella[64], V. Cepaitis[85], K. Cerny[178], A.S. Cerqueira[127], A. Cerri[XXXIX,113], L. Cerrito[117,118], F. Cerutti[19], B. Cervato[107,108], A. Cervelli[30], G. Cesarini[82], S.A. Cetin[126], P.M. Chabrillat[183], R. Chakkappai[99], S. Chakraborty[243], A. Chambers[91], J. Chan[19], W.Y. Chan[228], J.D. Chapman[46], E. Chapon[197], B. Chargeishvili[223], D.G. Charlton[23], C. Chauhan[195], Y. Che[164], S. Chekanov[7], G.A. Chelkov[I,66], B. Chen[226], B. Chen[241], H. Chen[164], H. Chen[43], J. Chen[210], J. Chen[215], M. Chen[182], S. Chen[139], S.J. Chen[164], X. Chen[210], X. Chen[XXXIV,16], Z. Chen[92], C.L. Cheng[246], H.C. Cheng[95], S. Cheong[216], A. Cheplakov[66], E. Cherepanova[169], R. Cherkaoui El Moursli[62], E. Cheu[8], K. Cheung[98], L. Chevalier[197], V. Chiarella[82], G. Chiarelli[113], G. Chiodini[105], A.S. Chisholm[23], A. Chitan[35], M. Chitishvili[239], M.V. Chizhov[XIX,66], K. Choi[12], Y. Chou[207], E.Y.S. Chow[168], K.L. Chu[245], M.C. Chu[95], X. Chu[15,166], Z. Chubinidze[82], J. Chudoba[193], J.J. Chwastowski[138], D. Cieri[162], K.M. Ciesla[136], V. Cindro[145], A. Ciocio[19], F. Cirotto[109,110], Z.H. Citron[245], M. Citterio[107], D.A. Ciubotaru[35], A. Clark[85], P.J. Clark[81], N. Clarke Hall[148], C. Clarry[230], S.E. Clawson[77], C. Clement[75,76], L. Clissa[30,29], Y. Coadou[154], M. Cobal[102,104], A. Coccaro[87], R.F. Coelho Barrue[186], R. Coelho Lopes De Sa[155], S. Coelli[107], L. S. Colangeli[230], B. Cole[69], P. Collado Soto[151], J. Collot[90], R. Coluccia[105,106], P. Conde Muiño[186,192], M.P. Connell[49], S.H. Connell[49], E.I. Conroy[182], M. Contreras Cossio[12], F. Conventi[XXXVI,109], A.M. Cooper-Sarkar[182], L. Corazzina[115,116], F. A. Corchia[30,29], A. Cordeiro Oudot Choi[207], L.D. Corpe[68], M. Corradi[115,116], F. Corriveau[XXVIII,156], A. Cortes-Gonzalez[228], M.J. Costa[239], F. Costanza[5], D. Costanzo[212], J. Couthures[5], G. Cowan[147], K. Cranmer[246], L. Cremer[78], D. Cremonini[30,29], S. Crépé-Renaudin[90], F. Crescioli[183], T. Cresta[111,112], M. Cristinziani[214], M. Cristoforetti[121,122], E. Critelli[148], V. Croft[169], G. Crosetti[72,71], A. Cueto[151], H. Cui[148], Z. Cui[8], B.M. Cunnett[219], W.R. Cunningham[89], F. Curcio[239], J. R. Curran[81], M.J. Da Cunha Sargedas De Sousa[87,86], J.V. Da Fonseca Pinto[128], C. Da Via[153], W. Dabrowski[136], T. Dado[64], S. Dahbi[221], T. Dai[158], D. Dal Santo[22], C. Dallapiccola[155], M. Dam[70], G. D'amen[43], V. D'Amico[161], J.R. Dandoy[57], M. D'Andrea[87,86], D. Dannheim[64], G. D'anniballe[113,114], M. Danninger[215], V. Dao[218], G. Darbo[87], S.J. Das[43], F. Dattola[77], S. D'Auria[107,108], A. D'Avanzo[109,110], T. Davidek[195], J. Davidson[243], I. Dawson[146], K. De[9], C. De Almeida Rossi[230], R. De Asmundis[109], N. De Biase[77], S. De Castro[30,29], N. De Groot[168], P. de Jong[169], H. De la Torre[170], A. De Maria[164], A. De Salvo[115], U. De Sanctis[117,118], F. De Santis[105,106], A. De Santo[219], J.B. De Vivie De Regie[90], J. Debevc[145], D.V. Dedovich[66], J. Degens[144], A.M. Deiana[73], J. Del Peso[151], L. Delagrange[183], F. Deliot[197], C.M. Delitzsch[78], M. Della Pietra[109,110], D. Della Volpe[85], A. Dell'Acqua[64], L. Dell'Asta[107,108], M. Delmastro[5], C.C. Delogu[87,86], P.A. Delsart[90], S. Demers[248], M. Demichev[66], S.P. Denisov[65], H. Denizli[XII,24], L. D'Eramo[68], D. Derendarz[138],

F. Derue[183], P. Dervan[XLII,144], A. M. Desai[1], K. Desch[31], F.A. Di Bello[87,86], A. Di Ciaccio[117,118], L. Di Ciaccio[5], A. Di Domenico[115,116], C. Di Donato[109,110], A. Di Girolamo[64], G. Di Gregorio[92], A. Di Luca[121,122], B. Di Micco[119,120], R. Di Nardo[119,120], K.F. Di Petrillo[67], M. Diamantopoulou[57], F.A. Dias[169], M.A. Diaz[199,200], A. R. Didenko[66], M. Didenko[239], S.D. Diefenbacher[19], E.B. Diehl[158], S. Díez Cornell[77], C. Diez Pardos[214], C. Dimitriadi[217], A. Dimitrievska[23], A. Dimri[218], Y. Ding[92], J. Dingfelder[31], T. Dingley[182], I-M. Dinu[35], S.J. Dittmeier[94], F. Dittus[64], M. Divisek[195], B. Dixit[144], F. Djama[154], T. Djobava[223], C. Doglioni[153,150], A. Dohnalova[41], Z. Dolezal[195], K. Domijan[136], K.M. Dona[67], M. Donadelli[130], B. Dong[159], J. Donini[68], A. D'Onofrio[109,110], M. D'Onofrio[144], J. Dopke[196], A. Doria[109], N. Dos Santos Fernandes[186], I.A. Dos Santos Luz[131], P. Dougan[153], M.T. Dova[142], A.T. Doyle[89], M.P. Drescher[84], E. Dreyer[245], I. Drivas-koulouris[11], M. Drnevich[173], D. Du[92], T.A. du Pree[169], Z. Duan[164], M. Dubau[5], F. Dubinin[66], M. Dubovsky[41], E. Duchovni[245], G. Duckeck[161], P. K. Duckett[148], O.A. Ducu[35], D. Duda[81], A. Dudarev[64], M.M. Dudek[138], E. R. Duden[33], M. D'uffizi[153], L. Duflot[99], M. Dührssen[64], I. Duminica[40], A.E. Dumitriu[35], M. Dunford[93], K. Dunne[75,76], A. Duperrin[154], H. Duran Yildiz[3], A. Durglishvili[223], G.I. Dyckes[19], M. Dyndal[136], B.S. Dziedzic[64], Z.O. Earnshaw[219], G.H. Eberwein[182], B. Eckerova[41], S. Eggebrecht[84], E. Egidio Purcino De Souza[131], G. Eigen[18], K. Einsweiler[19], T. Ekelof[237], P.A. Ekman[150], S. El Farkh[59], Y. El Ghazali[92], H. El Jarrari[56], A. El Moussaouy[58], D. Elitez[64], M. Ellert[237], F. Ellinghaus[247], T.A. Elliot[147], N. Ellis[64], J. Elmsheuser[43], M. Elsawy[171], M. Elsing[64], D. Emeliyanov[196], Y. Enari[132], S. Epari[160], D. Ernani Martins Neto[138], F. Ernst[64], M. Escalier[99], C. Escobar[239], E. Etzion[226], G. Evans[186,187], H. Evans[101], L.S. Evans[77], A. Ezhilov[65], S. Ezzarqtouni[58], F. Fabbri[30,29], L. Fabbri[30,29], G. Facini[148], V. Fadeyev[198], R.M. Fakhrutdinov[65], D. Fakoudis[152], S. Falciano[115], L.F. Falda Ulhoa Coelho[186], F. Fallavollita[162], G. Falsetti[72,71], J. Faltova[195], C. Fan[238], K. Y. Fan[96], Y. Fan[15], Y. Fang[15,166], M. Fanti[107,108], M. Faraj[102,103], Z. Farazpay[149], A. Farbin[9], A. Farilla[119], K. Farman[221], T. Farooque[159], J. N. Farr[248], M. S. Farrington[91], S.M. Farrington[196,81], F. Fassi[62], D. Fassouliotis[10], L. Fayard[99], P. Federic[195], P. Federicova[193], O.L. Fedin[I,65], M. Feickert[246], L. Feligioni[154], D.E. Fellers[19], C. Feng[208], Y. Feng[15], Z. Feng[169], M.J. Fenton[235], L. Ferencz[77], B. Fernandez Barbadillo[143], P. Fernandez Martinez[100], M.J.V. Fernoux[154], J. Ferrando[143], A. Ferrari[237], P. Ferrari[169,168], R. Ferrari[111], D. Ferrere[85], C. Ferretti[158], M. P. Fewell[1], D. Fiacco[115,116], F. Fiedler[152], P. Fiedler[194], S. Filimonov[66], M.S. Filip[XX,35], A. Filipčič[145], E.K. Filmer[231], F. Filthaut[168], M.C.N. Fiolhais[III,186,188], L. Fiorini[239], W.C. Fisher[159], T. Fitschen[153], P. M. Fitzhugh[197], I. Fleck[214], P. Fleischmann[158], T. Flick[247], M. Flores[XXXIII,50], L.R. Flores Castillo[95], L. Flores Sanz De Acedo[64], F.M. Follega[121,122], N. Fomin[46], J.H. Foo[230], A. Formica[197], A.C. Forti[153], E. Fortin[64], A.W. Fortman[19], L. Foster[19], L. Fountas[IX,10], D. Fournier[99], H. Fox[143], P. Francavilla[113,114], S. Francescato[91], S. Franchellucci[85], M. Franchini[30,29], S. Franchino[93], D. Francis[64], L. Franco[168], L. Franconi[77], M. Franklin[91], G. Frattari[33], Y.Y. Frid[226], J. Friend[89], N. Fritzsche[64], A. Froch[85], D. Froidevaux[64], J.A. Frost[196], Y. Fu[159], S. Fuenzalida Garrido[205], M. Fujimoto[218], K. Y. Fung[95], E. Furtado De Simas Filho[131], M. Furukawa[228], J. Fuster[239], A. Gaa[84], A. Gabrielli[30,29], A. Gabrielli[230], P. Gadow[64], G. Gagliardi[87,86], L.G. Gagnon[19], S. Gaid[134], S. Galantzan[226], J. Gallagher[1], E.J. Gallas[182], A.L. Gallen[237], B.J. Gallop[196], K.K. Gan[175], S. Ganguly[228], Y. Gao[81], A. Garabaglu[207], F.M. Garay Walls[199,200], C. García[239], A. Garcia Alonso[169], A.G. Garcia Caffaro[248], J.E. García Navarro[239], M. A. Garcia Ruiz[28], M. Garcia-Sciveres[19], G.L. Gardner[184], R.W. Gardner[67], N. Garelli[234], R.B. Garg[216], J.M. Gargan[46], C.A. Garner[230], C.M. Garvey[47], V. K. Gassmann[234], G. Gaudio[111], V. Gautam[14], P. Gauzzi[115,116], J. Gavranovic[145], I.L. Gavrilenko[186], A. Gavrilyuk[65], C. Gay[240], G. Gaycken[179], E.N. Gazis[11], A. Gekow[175], C. Gemme[87], M.H. Genest[90], A. D. Gentry[167], S. George[147], T. Geralis[74], A. A. Gerwin[176], P. Gessinger-Befurt[64], M.E. Geyik[247], M. Ghani[243], K. Ghorbanian[146], A. Ghosal[214], A. Ghosh[235], A. Ghosh[8], B. Giacobbe[30], S. Giagu[115,116], T. Giani[169], A. Giannini[92], S.M. Gibson[147], M. Gignac[198], D.T. Gil[137], A.K. Gilbert[136], B.J. Gilbert[69], D. Gillberg[57], G. Gilles[169], D.M. Gingrich[XXXV,2], M.P. Giordani[102,104], P.F. Giraud[197], G. Giugliarelli[102,104], D. Giugni[107], F. Giuli[117,118], I. Gkialas[IX,10], L.K. Gladilin[65], C. Glasman[151], M. Glazewska[22], R. M. Gleason[235], G. Glemža[77], M. Glisic[179], I. Gnesi[72], Y. Go[43], M. Goblirsch-Kolb[64], B. Gocke[78], D. Godin[160], B. Gokturk[24], S. Goldfarb[157], T. Golling[85], M.G.D. Gololo[49], D. Golubkov[65], J.P. Gombas[159], A. Gomes[186,187], G. Gomes Da Silva[214], A.J. Gomez Delegido[64], R. Gonçalo[186], L. Gonella[23], A. Gongadze[224], F. Gonnella[23], J.L. Gonski[216], R.Y. González Andana[81], S. González de la Hoz[239], M. V. Gonzalez Rodrigues[77], R. Gonzalez Suarez[237], S. Gonzalez-Sevilla[85], L. Goossens[64], B. Gorini[64], E. Gorini[105,106], A. Gorišek[145], T.C. Gosart[184], A.T. Goshaw[80], M.I. Gostkin[66], S. Goswami[177], C.A. Gottardo[64], S. A. Gotz[161], M. Gouighri[59], A.G. Goussiou[207], N. Govender[49], R. P. Grabarczyk[182], I. Grabowska-Bold[136], K. Graham[57], E. Gramstad[181], S. Grancagnolo[105,106], C.M. Grant[1], P.M. Gravila[39], F.G. Gravili[105,106], H.M. Gray[19], M. Greco[162], M. J. Green[1], C. Grefe[31], A. S. Grefsrud[18], I.M. Gregor[77], K.T. Greif[235], P. Grenier[216], S.G. Grewe[162], A.A. Grillo[198], K. Grimm[45], S. Grinstein[XXIV,14], J.-F. Grivaz[99], E. Gross[245], J. Grosse-Knetter[84], L. Guan[158], G. Guerrieri[64], R. Guevara[181], R. Gugel[152], J.A.M. Guhit[158], A. Guida[21], E. Guilloton[243], S. Guindon[64], F. Guo[15,166], J. Guo[210], L. Guo[77], L. Guo[XXII,165], Y. Guo[158], Y. Guo[69], A. Gupta[78], R. Gupta[185], S. Gupta[33], S. Gurbuz[31], S.S. Gurdasani[77], G. Gustavino[115,116], P. Gutierrez[176], L.F. Gutierrez Zagazeta[184], M. Gutsche[79], C. Gutschow[148], C. Gwenlan[182], C.B. Gwilliam[144], E.S. Haaland[181], A. Haas[173], M. Habedank[89], C. Haber[19], H.K. Hadavand[9], A. Haddad[68], A. Hadef[79], A.I. Hagan[143], J. J. Hahn[214], E.H. Haines[148], M. Haleem[242], J. Haley[177], G.D. Hallewell[154], J.A. Hallford[77], K. Hamano[241], H. Hamdaoui[237], M. Hamer[31], S. E. D. Hammoud[99], E.J. Hampshire[147], J. Han[208], L. Han[164], L. Han[92], S. Han[15], K. Hanagaki[132], M. Hance[198], D.A. Hangal[69], H. Hanif[215], M.D. Hank[184], J.B. Hansen[70], P.H. Hansen[70], T. Harenberg[247], S. Harkusha[249], M.L. Harris[155], Y.T. Harris[31], J. Harrison[14], N.M. Harrison[175], P.F. Harrison[243], M. L. E. Hart[148], N.M. Hartman[162], N.M. Hartmann[161], R. Z. Hasan[147,196], Y. Hasegawa[213], F. Haslbeck[182], S. Hassan[18], R. Hauser[159], M. Haviernik[195], C.M. Hawkes[23], R.J. Hawkings[64], Y. Hayashi[228], D. Hayden[159], C. Hayes[158], R.L. Hayes[169], C.P. Hays[182], J.M. Hays[146], H.S. Hayward[144], M. He[15,166], Y. He[77], Y. He[148], N.B. Heatley[146], V. Hedberg[150], J. Heilman[57], S. Heim[77], T. Heim[19], J.J. Heinrich[179], L. Heinrich[162], J. Hejbal[193], M. Helbig[79], A. Held[246], S. Hellesund[18], C.M. Helling[240], S. Hellman[75,76], A.M. Henriques Correia[64], H. Herde[150], Y. Hernández Jiménez[218], L.M. Herrmann[31], T. Herrmann[79], G. Herten[83], R. Hertenberger[161], L. Hervas[64], M.E. Hesping[152], N.P. Hessey[231], J. Hessler[162], M. Hidaoui[59], N. Hidic[195], E. Hill[230], T. S. Hillersoy[18], S.J. Hillier[23], J.R. Hinds[159], F. Hinterkeuser[31], M. Hirose[180], S. Hirose[233], D. Hirschbuehl[247], T.G. Hitchings[153], B. Hiti[145], J. Hobbs[218], R. Hobincu[38], N. Hod[245], A.M. Hodges[238], M.C. Hodgkinson[212], B.H. Hodkinson[182], A. Hoecker[64], D. D. Hofer[158], J. Hofer[239], J. Hofner[152], M. Holzbock[64], L.B.A.H. Hommels[46], V. Homsak[182], B.P. Honan[153], J. J. Hong[101], T.M. Hong[185], B.H. Hooberman[238], W.H. Hopkins[7], M. C. Hoppesch[238], Y. Horii[163], M. E. Horstmann[162], S. Hou[221], M. R. Housenga[238], J. Howarth[89], J. Hoya[7], M. Hrabovsky[178], T. Hryn'ova[5], P.J. Hsu[98], S.-C. Hsu[207], T. Hsu[99], M. Hu[19], Q. Hu[92], S. Huang[46], X. Huang[15,166], Y. Huang[195], Y. Huang[165], Y.

Huang[15], Z. Huang[99], Z. Hubacek[194], F. Huegging[31], T.B. Huffman[182], M. Hufnagel Maranha De Faria[127], C. A. Hugli[77], M. Huhtinen[64], S.K. Huiberts[181], R. Hulsken[156], C. E. Hultquist[19], D.L. Humphreys[155], N. Huseynov[13], J. Huston[159], J. Huth[91], L. Huth[77], R. Hyneman[8], G. Iacobucci[85], G. Iakovidis[43], L. Iconomidou-Fayard[99], J. P. Iddon[64], P. Iengo[109,110], Y. Iiyama[228], T. Iizawa[228], Y. Ikegami[132], D. Iliadis[227], N. Ilic[230], H. Imam[58], G. Inacio Goncalves[130], S. A. Infante Cabanas[201], T. Ingebretsen Carlson[75,76], J. M. Inglis[146], G. Introzzi[111,112], M. Iodice[119], V. Ippolito[115,116], R. K. Irwin[144], M. Ishino[228], W. Islam[246], C. Issever[21], S. Istin[XLI,24], K. Itabashi[180], H. Ito[244], R. Iuppa[121,122], A. Ivina[245], V. Izzo[109], P. Jacka[194], P. Jackson[1], P. Jain[77], K. Jakobs[83], T. Jakoubek[245], J. Jamieson[89], W. Jang[228], S. Jankovych[195], M. Javurkova[155], P. Jawahar[153], L. Jeanty[179], J. Jejelava[XXXI,222], P. Jenni[VI,83], C.E. Jessiman[57], C. Jia[208], H. Jia[240], J. Jia[218], X. Jia[162,166], Z. Jia[164], C. Jiang[81], Q. Jiang[96], S. Jiggins[77], M. Jimenez Ortega[239], J. Jimenez Pena[14], S. Jin[164], A. Jinaru[35], O. Jinnouchi[206], P. Johansson[212], K.A. Johns[8], J.W. Johnson[198], F. A. Jolly[77], D.M. Jones[219], E. Jones[77], K.S. Jones[9], P. Jones[46], R.W.L. Jones[143], T.J. Jones[144], H.L. Joos[84], R. Joshi[175], J. Jovicevic[17], X. Ju[19], J.J. Junggeburth[64], T. Junkermann[93], A. Juste Rozas[XXIV,14], M.K. Juzek[138], S. Kabana[204], A. Kaczmarska[138], S. A. Kadir[216], M. Kado[162], H. Kagan[175], M. Kagan[216], A. Kahn[184], C. Kahra[152], T. Kaji[228], E. Kajomovitz[225], N. Kakati[245], N. Kakoty[14], I. Kalaitzidou[83], S. Kandel[9], N. Kanellos[11], N.J. Kang[198], D. Kar[56], E. Karentzos[31], K. Karki[9], O. Karkout[169], S.N. Karpov[66], Z.M. Karpova[66], V. Kartvelishvili[143,223], A.N. Karyukhin[65], E. Kasimi[227], J. Katzy[77], S. Kaur[57], K. Kawade[213], M.P. Kawale[176], C. Kawamoto[139], T. Kawamoto[92], E.F. Kay[64], S. Kazakos[159], V.F. Kazanin[65], J.M. Keaveney[47], R. Keeler[241], G.V. Kehris[91], J.S. Keller[57], J. M. Kelly[241], J.J. Kempster[219], O. Kepka[193], J. Kerr[232], B.P. Kerridge[196], B.P. Kerševan[145], L. Keszeghova[41], R. A. Khan[185], A. Khanov[177], A.G. Kharlamov[65], T. Kharlamova[65], E.E. Khoda[207], M. Kholodenko[186], T.J. Khoo[21], G. Khoriauli[242], Y. Khoulaki[58], Y.A.R. Khwaira[183], B. Kibirige[56], D. Kim[7], D.W. Kim[20], Y.K. Kim[67], N. Kimura[148], M.K. Kingston[84], A. Kirchhoff[84], C. Kirfel[31], F. Kirfel[31], J. Kirk[196], A.E. Kiryunin[162], S. Kita[233], O. Kivernyk[31], M. Klassen[234], C. Klein[57], L. Klein[242], M.H. Klein[73], S.B. Klein[85], U. Klein[144], A. Klimentov[43], T. Klioutchnikova[64], P. Kluit[169], S. Kluth[162], E. Kneringer[123], T.M. Knight[230], A. Knue[78], M. Kobel[79], D. Kobylianskii[245], S.F. Koch[182], M. Kocian[216], P. Kodyš[195], D.M. Koeck[179], T. Koffas[57], O. Kolay[79], I. Koletsou[5], T. Komarek[138], K. Köneke[84], A.X.Y. Kong[1], T. Kono[174], N. Konstantinidis[148], P. Kontaxakis[85], B. Konya[150], R. Kopeliansky[69], S. Koperny[136], K. Korcyl[138], K. Kordas[IV,227], A. Korn[148], S. Korn[84], I. Korolkov[14], N. Korotkova[65], B. Kortman[169], O. Kortner[162], S. Kortner[162], W.H. Kostecka[170], M. Kostov[41], V.V. Kostyukhin[214], A. Kotsokechagia[64], A. Kotwal[80], A. Koulouris[64], A. Kourkoumeli-Charalampidi[111,112], C. Kourkoumelis[10], E. Kourlitis[162], O. Kovanda[179], R. Kowalewski[241], W. Kozanecki[179], A.S. Kozhin[65], V.A. Kramarenko[65], G. Kramberger[145], P. Kramer[31], M.W. Krasny[183], A. Krasznahorkay[155], A. C. Kraus[170], J.W. Kraus[247], J.A. Kremer[77], N. B. Krengel[214], T. Kresse[79], L. Kretschmann[247], J. Kretzschmar[144], P. Krieger[230], K. Krizka[23], K. Kroeninger[78], H. Kroha[162], J. Kroll[193], J. Kroll[184], K.S. Krowpman[159], U. Kruchonak[66], H. Krüger[31], N. Krumnack[125], M.C. Kruse[80], O. Kuchinskaia[66], S. Kuday[3], S. Kuehn[64], R. Kuesters[83], T. Kuhl[77], V. Kukhtin[66], Y. Kulchitsky[66], S. Kuleshov[202,200], J. Kull[1], E. V. Kumar[161], M. Kumar[56], N. Kumari[77], P. Kumari[232], A. Kupco[193], A. Kupich[65], O. Kuprash[83], H. Kurashige[135], L.L. Kurchaninov[231], O. Kurdysh[5], A. Kurova[65], M. Kuze[206], A.K. Kvam[155], J. Kvita[178], N.G. Kyriacou[207], M. Laassiri[43], C. Lacasta[239], F. Lacava[115,116], H. Lacker[21], D. Lacour[183], N.N. Lad[148], E. Ladygin[66], A. Lafarge[68], B. Laforge[183], T. Lagouri[248], F.Z. Lahbabi[58], S. Lai[84,64], W. S. Lai[148], J.E. Lambert[241], S. Lammers[101], W. Lampl[8], C. Lampoudis[IV,227], G. Lamprinoudis[242], A.N. Lancaster[170], E. Lançon[43], U. Landgraf[83], M.P.J. Landon[146], V.S. Lang[83], A.J. Lankford[235], F. Lanni[64], K. Lantzsch[31], A. Lanza[111], M. Lanzac Berrocal[239], J.F. Laporte[197], T. Lari[107], D. Larsen[18], L. Larson[12], F. Lasagni Manghi[30], M. Lassnig[64], S.D. Lawlor[212], R. Lazaridou[235], M. Lazzaroni[107,108], E. T. T. Le[235], H. D. M. Le[159], E.M. Le Boulicaut[248], L.T. Le Pottier[19], B. Leban[30,29], F. Ledroit-Guillon[90], T.F. Lee[232], L.L. Leeuw[49], M. Lefebvre[241], C. Leggett[19], G. Lehmann Miotto[64], M. Leigh[85], W.A. Leight[155], W. Leinonen[168], A. Leisos[XXI,227], M.A.L. Leite[129], C.E. Leitgeb[21], R. Leitner[195], K.J.C. Leney[73], T. Lenz[31], S. Leone[113], C. Leonidopoulos[81], A. Leopold[217], J.H. Lepage Bourbonnais[57], R. Les[159], C.G. Lester[46], M. Levchenko[65], J. Levêque[5], L.J. Levinson[245], G. Levrini[30,29], M.P. Lewicki[138], C. Lewis[207], D.J. Lewis[5], L. Lewitt[212], A. Li[43], B. Li[208], C. Li[158], C-Q. Li[162], H. Li[208], H. Li[153], H. Li[16], H. Li[92], H. Li[208], J. Li[210], K. Li[15], L. Li[210], R. Li[248], S. Li[15,166], S. Li[211,210], T. Li[6], X. Li[156], Y. Li[15], Z. Li[228], Z. Li[15,166], Z. Li[92], S. Liang[15,166], Z. Liang[15], M. Liberatore[197], B. Liberti[117], G. B. Libotte[130], K. Lie[97], J. Lieber Marin[131], H. Lien[101], H. Lin[158], S. F. Lin[218], L. Linden[161], R.E. Lindley[8], J.H. Lindon[64], J. Ling[91], E. Lipeles[184], A. Lipniacka[18], A. Lister[240], J.D. Little[101], B. Liu[15], B.X. Liu[165], D. Liu[211], D. Liu[198], E. H. L. Liu[23], J.K.K. Liu[173], K. Liu[211], K. Liu[211,210], M. Liu[92], M.Y. Liu[92], P. Liu[15], Q. Liu[216], S. Liu[218], X. Liu[92], X. Liu[208], Y. Liu[165,166], Y. Liu[238], Y.L. Liu[208], Y.W. Liu[92], Z. Liu[XI,99], S.L. Lloyd[146], E.M. Lobodzinska[77], P. Loch[8], E. Lodhi[230], K. Lohwasser[212], E. Loiacono[77], J. D. Lomas[23], J.D. Long[69], I. Longarini[235], R. Longo[238], A. Lopez Solis[14], N.A. Lopez-canelas[8], N. Lorenzo Martinez[5], A.M. Lory[161], M. Losada[171], G. Löschcke Centeno[5], X. Lou[75,76], X. Lou[15,166], A. Lounis[99], P.A. Love[143], M. Lu[99], S. Lu[184], Y.J. Lu[221], H.J. Lubatti[207], C. Luci[115,116], F.L. Lucio Alves[164], F. Luehring[101], B. S. Lunday[184], O. Lundberg[217], J. Lunde[64], N.A. Luongo[7], M.S. Lutz[64], A.B. Lux[32], D. Lynn[43], R. Lysak[193], V. Lysenko[194], E. Lytken[150], V. Lyubushkin[66], T. Lyubushkina[66], M.M. Lyukova[218], H. Ma[43], K. Ma[92], L.L. Ma[208], W. Ma[92], Y. Ma[177], J.C. MacDonald[152], P.C. Machado De Abreu Farias[131], D. Macina[64], R. Madar[68], T. Madula[148], J. Maeda[135], T. Maeno[43], P.T. Mafa[X,49], H. Maguire[212], M. Maheshwari[46], V. Maiboroda[99], A. Maio[186,187,189], K. Maj[136], O. Majersky[77], S. Majewski[179], R. Makhmanazarov[65], N. Makovec[99], V. Maksimovic[17], B. Malaescu[183], J. Malamant[181], Pa. Malecki[138], V.P. Maleev[65], F. Malek[XV,90], M. Mali[145], D. Malito[147], U. Mallik[XLII,124], A. Maloizel[6], S. Maltezos[11], A. Malvezzi Lopes[130], S. Malyukov[66], J. Mamuzic[145], G. Mancini[82], M. N. Mancini[33], G. Manco[111,112], J.P. Mandalia[146], S.S. Mandarry[219], I. Mandić[145], L. Manhaes de Andrade Filho[127], I.M. Maniatis[245], J. Manjarres Ramos[141], D.C. Mankad[245], A. Mann[161], T. Manoussos[64], M.N. Mantinan[67], S. Manzoni[64], L. Mao[210], X. Mapekula[49], A. Marantis[227], R.R. Marcelo Gregorio[146], G. Marchiori[6], C. Marcon[107], E. Maricic[17], M. Marinescu[77], S. Marium[77], M. Marjanovic[176], A. Markhoos[83], M. Markovitch[99], M. K. Maroun[155], M. C. Marr[215], G. T. Marsden[153], E.J. Marshall[143], Z. Marshall[19], S. Marti-Garcia[239], J. Martin[148], T.A. Martin[196], V.J. Martin[81], B. Martin dit Latour[18], L. Martinelli[115,116], M. Martinez[XXIV,14], P. Martinez Agullo[239], V.I. Martinez Outschoorn[155], P. Martinez Suarez[64], S. Martin-Haugh[196], G. Martinovicova[195], V.S. Martoiu[35], A.C. Martyniuk[148], A. Marzin[64], D. Mascione[121,122], L. Masetti[152], J. Masik[153], A.L. Maslennikov[66], S.L. Mason[69], P. Massarotti[109,110], P. Mastrandrea[113,114], A. Mastroberardino[72,71], T. Masubuchi[180], T.T. Mathew[179], J. Matousek[195], D.M. Mattern[78], K. Mauer[77], J. Maurer[35], T. Maurin[89], A.J. Maury[99], B. Maček[145], C. Mavungu Tsava[154], D.A. Maximov[65], A. E. May[153], E. Mayer[68], R. Mazini[56], I. Maznas[170], S.M. Mazza[198], E. Mazzeo[64], J.P. Mc Gowan[241], S.P. Mc Kee[158], C.A. Mc

Lean[7], C.C. McCracken[240], E.F. McDonald[157], A.E. McDougall[169], L. F. Mcelhinney[143], J.A. Mcfayden[219], R.P. McGovern[184], R.P. Mckenzie[56], T.C. Mclachlan[77], D.J. Mclaughlin[148], S.J. McMahon[196], C.M. Mcpartland[144], R.A. McPherson[XXVIII,241], S. Mehlhase[161], A. Mehta[144], D. Melini[239], B.R. Mellado Garcia[56], A.H. Melo[84], F. Meloni[77], A.M. Mendes Jacques Da Costa[153], L. Meng[143], S. Menke[162], M. Mentink[64], E. Meoni[72,71], G. Mercado[170], S. Merianos[227], C. Merlassino[102,104], C. Meroni[107,108], J. Metcalfe[7], A.S. Mete[7], E. Meuser[152], C. Meyer[101], J-P. Meyer[197], Y. Miao[164], R.P. Middleton[196], M. Mihovilovic[99], L. Mijović[81], G. Mikenberg[245], M. Mikestikova[193], M. Mikuž[145], H. Mildner[152], A. Milic[64], D.W. Miller[67], E. H. Miller[216], A. Milov[245], D.A. Milstead[75,76], T. Min[164], A.A. Minaenko[65], I.A. Minashvili[223], A.I. Mincer[173], B. Mindur[136], M. Mineev[66], Y. Mino[139], L.M. Mir[14], M. Miralles Lopez[89], M. Mironova[19], M. Missio[68], A. Mitra[243], V.A. Mitsou[239], Y. Mitsumori[163], O. Miu[230], P.S. Miyagawa[146], T. Mkrtchyan[64], M. Mlinarevic[148], T. Mlinarevic[148], M. Mlynarikova[195], L. Mlynarska[136], C. Mo[210], S. Mobius[22], M. H. Mohamed Farook[167], S. Mohapatra[69], M.F. Mohd Soberi[81], S. Mohiuddin[177], G. Mokgatitswane[56], L. Moleri[245], U. Molinatti[182], L.G. Mollier[22], B. Mondal[193], S. Mondal[194], K. Mönig[77], E. Monnier[154], L. Monsonis Romero[239], J. Montejo Berlingen[14], A. Montella[75,76], M. Montella[175], F. Montereali[119,120], F. Monticelli[142], S. Monzani[102,104], A. Morancho Tarda[70], N. Morange[99], A.L. Moreira De Carvalho[77], M. Moreno Llácer[239], C. Moreno Martinez[85], J.M. Moreno Perez[28], P. Morettini[87], S. Morgenstern[64], M. Morii[91], M. Morinaga[228], M. Moritsu[140], F. Morodei[115,116], P. Moschovakos[64], B. Moser[83], M. Mosidze[223], T. Moskalets[73], P. Moskvitina[168], J. Moss[45], P. Moszkowicz[136], T. Motta Quirino[130], A. Moussa[61], Y. Moyal[245], H. Moyano Gomez[14], E.J.W. Moyse[155], T.G. Mroz[138], S. Muanza[154], M. Mucha[31], J. Mueller[185], R. Müller[64], G.A. Mullier[237], A.J. Mullin[46], J.J. Mullin[80], A.C. Mullins[73], A.E. Mulski[91], D.P. Mungo[230], D. Munoz Perez[239], F.J. Munoz Sanchez[153], W.J. Murray[243,196], M. Muškinja[145], C. Mwewa[77], A.G. Myagkov[I,65], A.J. Myers[9], G. Myers[158], M. Myska[194], B.P. Nachman[216], K. Nagai[182], K. Nagano[132], R. Nagasaka[228], J.L. Nagle[XXXVIII,43], E. Nagy[154], A.M. Nairz[64], Y. Nakahama[132], K. Nakamura[132], K. Nakkalil[6], A. Nandi[94], H. Nanjo[180], E.A. Narayanan[73], Y. Narukawa[228], I. Naryshkin[65], L. Nasella[107,108], S. Nasri[172], C. Nass[31], G. Navarro[27], A. Nayaz[21], P.Y. Nechaeva[65], S. Nechaeva[30,29], F. Nechansky[193], L. Nedic[182], T.J. Neep[23], A. Negri[111,112], M. Negrini[30], C. Nellist[169], C. Nelson[156], K. Nelson[158], S. Nemecek[193], M. Nessi[VII,64], M.S. Neubauer[238], J. Newell[144], P.R. Newman[23], Y.W.Y. Ng[238], B. Ngair[171], H.D.N. Nguyen[160], J.D. Nichols[176], R.B. Nickerson[182], R. Nicolaidou[197], J. Nielsen[198], M. Niemeyer[84], J. Niermann[64], N. Nikiforou[64], V. Nikolaenko[I,65], I. Nikolic-Audit[183], P. Nilsson[43], I. Ninca[77], G. Ninio[226], A. Nisati[115], R. Nisius[162], N. Nitika[245], E.K. Nkadimeng[48], T. Nobe[228], D. Noll[216], T. Nommensen[220], M.B. Norfolk[212], B.J. Norman[57], L.C. Nosler[19], M. Noury[58], J. Novak[145], T. Novak[145], R. Novotny[194], L. Nozka[178], K. Ntekas[235], D. Ntounis[216], N.M.J. Nunes De Moura Junior[128], J. Ocariz[183], I. Ochoa[186], S. Oerdek[XXV,77], J.T. Offermann[67], A. Ogrodnik[138], A. Oh[153], C.C. Ohm[217], H. Oide[132], M.L. Ojeda[64], Y. Okumura[228], L.F. Oleiro Seabra[186], I. Oleksiyuk[85], G. Oliveira Correa[14], D. Oliveira Damazio[43], J.L. Oliver[1], R. Omar[101], Ö.O. Öncel[83], A.P. O'Neill[22], A. Onofre[V,186,190], P.U.E. Onyisi[12], M.J. Oreglia[67], D. Orestano[119,120], R. Orlandini[119,120], R.S. Orr[230], L.M. Osojnak[69], Y. Osumi[163], G. Otero y Garzon[44], H. Otono[140], M. Ouchrif[61], F. Ould-Saada[181], T. Ovsiannikova[207], M. Owen[89], R.E. Owen[196], V.E. Ozcan[24], F. Ozturk[138], N. Ozturk[9], S. Ozturk[126], H.A. Pacey[182], K. Pachal[231], A. Pacheco Pages[14], C. Padilla Aranda[14], G. Padovano[115,116], S. Pagan Griso[19], J. Pampel[31], J. Pan[248], D.K. Panchal[12], C.E. Pandini[90], J.G. Panduro Vazquez[196], H.D. Pandya[1], H. Pang[197], P. Pani[77], G. Panizzo[102,104], L. Panwar[183], L. Paolozzi[85], S. Parajuli[238], A. Paramonov[7], C. Paraskevopoulos[82], D. Paredes Hernandez[96], S.R. Paredes Saenz[81], A. Pareti[111,112], K.R. Park[69], T.H. Park[162], F. Parodi[87,86], J.A. Parsons[69], U. Parzefall[83], B. Pascual Dias[68], L. Pascual Dominguez[151], E. Pasqualucci[115], S. Passaggio[87], F. Pastore[147], P. Patel[138], U.M. Patel[80], J.R. Pater[153], T. Pauly[64], F. Pauwels[195], C.I. Pazos[234], M. Pedersen[181], R. Pedro[186], S.V. Peleganchuk[65], O. Penc[193], S. Peng[16], G. D. Penn[248], K.E. Penski[161], M. Penzin[65], B.S. Peralva[130], A.P. Pereira Peixoto[207], L. Pereira Sanchez[216], D.V. Perepelitsa[XXXVIII,43], G. Perera[155], E. Perez Codina[64], M. Perganti[11], H. Pernegger[64], S. Perrella[115,116], K. Peters[77], R.F.Y. Peters[153], B.A. Petersen[64], T.C. Petersen[70], E. Petit[154], V. Petousis[194], A. R. Petri[107,108], C. Petridou[IV,227], T. Petru[195], M. Pettee[19], A. Petukhov[126], K. Petukhova[64], R. Pezoa[205], L. Pezzotti[30,29], G. Pezzullo[248], L. Pfaffenbichler[64], A. J. Pfleger[123], T.M. Pham[246], T. Pham[157], P.W. Phillips[196], G. Piacquadio[218], E. Pianori[19], F. Piazza[179], R. Piegaia[44], D. Pietreanu[35], A.D. Pilkington[153], M. Pinamonti[102,104], J.L. Pinfold[2], G. Pinheiro Matos[69], B.C. Pinheiro Pereira[186], J. Pinol Bel[14], A. E. Pinto Pinoargote[183], L. Pintucci[102,104], K. M. Piper[219], A. Pirttikoski[85], D.A. Pizzi[57], L. Pizzimento[96], A. Plebani[46], M.-A. Pleier[43], V. Pleskot[195], E. Plotnikova[66], G. Poddar[146], R. Poettgen[150], L. Poggioli[183], S. Polacek[195], G. Polesello[111], A. Poley[215], A. Polini[30], C.S. Pollard[243], Z.B. Pollock[175], E. Pompa Pacchi[176], N. I. Pond[148], D. Ponomarenko[101], L. Pontecorvo[64], S. Popa[34], G.A. Popeneciu[37], A. Poreba[64], D.M. Portillo Quintero[231], S. Pospisil[194], M. A. Postill[212], P. Postolache[36], K. Potamianos[243], P.A. Potepa[136], I.N. Potrap[66], C.J. Potter[46], H. Potti[220], J. Poveda[239], M.E. Pozo Astigarraga[64], R. Pozzi[64], A. Prades Ibanez[117,118], S.R. Pradhan[212], J. Pretel[241], D. Price[153], M. Primavera[105], L. Primomo[102,104], M.A. Principe Martin[151], R. Privara[178], T. Procter[137], M.L. Proffitt[207], N. Proklova[184], K. Prokofiev[97], G. Proto[162], J. Proudfoot[7], M. Przybycien[136], W.W. Przygoda[137], A. Psallidas[74], J.E. Puddefoot[212], D. Pudzha[82], H. I. Purnell[1], D. Pyatiizbyantseva[168], J. Qian[158], R. Qian[159], D. Qichen[182], Y. Qin[14], T. Qiu[81], A. Quadt[84], M. Queitsch-Maitland[153], G. Quetant[85], R.P. Quinn[240], G. Rabanal Bolanos[91], D. Rafanoharana[162], F. Raffaeli[117,118], F. Ragusa[107,108], J.L. Rainbolt[67], S. Rajagopalan[43], E. Ramakoti[66], L. Rambelli[87,86], I.A. Ramirez-Berend[57], K. Ran[158,166], D. S. Rankin[184], N.P. Rapheeha[56], H. Rasheed[35], A. Rastogi[19], S. Rave[152], S. Ravera[87,86], B. Ravina[64], I. Ravinovich[245], M. Raymond[64], A.L. Read[181], N.P. Readioff[212], D.M. Rebuzzi[111,112], A. S. Reed[89], K. Reeves[33], D. Reikher[64], A. Rej[78], C. Rembser[64], H. Ren[92], M. Renda[35], F. Renner[77], A.G. Rennie[89], M. Repik[85], A.L. Rescia[87,86], S. Resconi[107], M. Ressegotti[87,86], S. Rettie[169], W.F. Rettie[57], M. M. Revering[46], E. Reynolds[19], O.L. Rezanova[66], P. Reznicek[195], H. Riani[61], N. Ribaric[80], B. Ricci[102,104], E. Ricci[121,122], R. Richter[162], S. Richter[75,76], E. Richter-Was[137], M. Ridel[183], S. Ridouani[61], P. Rieck[173], P. Riedler[64], E.M. Riefel[75,76], J. O. Rieger[169], M. Rijssenbeek[218], M. Rimoldi[64], L. Rinaldi[30,29], P. Rincke[237,84], G. Ripellino[237], I. Riu[14], J.C. Rivera Vergara[241], F. Rizatdinova[177], E. Rizvi[146], B.R. Roberts[19], S.S. Roberts[198], D. Robinson[46], A. Robson[89], A. Rocchi[117,118], C. Roda[113,114], F.A. Rodriguez[170], S. Rodriguez Bosca[64], Y. Rodriguez Garcia[27], A.M. Rodríguez Vera[170], S. Roe[64], J.T. Roemer[64], O. Røhne[181], R.A. Rojas[64], C.P.A. Roland[183], A. Romaniouk[123], E. Romano[111,112], M. Romano[30], A.C. Romero Hernandez[238], N. Rompotis[144], L. Roos[183], S. Rosati[115], B.J. Rosser[67], E. Rossi[182], E. Rossi[109,110], L.P. Rossi[91], L. Rossini[83], R. Rosten[175], M. Rotaru[35], D. Rousseau[99], D. Rousso[77], S. Roy-Garand[230], A. Rozanov[154], Z. M. A. Rozario[89], Y. Rozen[225], A. Rubio Jimenez[239], V.H. Ruelas Rivera[21], T.A. Ruggeri[1], A. Ruggiero[182], A. Ruiz-Martinez[239], A. Rummler[64], G.B. Rupnik Boero[64], Z. Rurikova[83], N.A. Rusakovich[66], S. Ruscelli[78], H.L.

Russell[241], G. Russo[115,116], J.P. Rutherfoord[8], S. Rutherford Colmenares[46], M. Rybar[195], P. Rybczynski[136], A. Ryzhov[73], J.A. Sabater Iglesias[85], H.F-W. Sadrozinski[198], F. Safai Tehrani[115], S. Saha[1], M. Sahinsoy[126], B. Sahoo[245], A. Saibel[239], B. T. Saifuddin[176], M. Saimpert[197], G.T. Saito[129], M. Saito[228], T. Saito[228], A. Sala[107,108], A. Salnikov[216], J. Salt[239], A. Salvador Salas[226], F. Salvatore[219], A. Salzburger[64], D. Sammel[83], E. Sampson[143], D. Sampsonidis[IV,227], D. Sampsonidou[179], M.A.A. Samy[89], J. Sánchez[239], V. Sanchez Sebastian[239], H. Sandaker[181], C.O. Sander[77], J.A. Sandesara[246], M. Sandhoff[247], C. Sandoval[28], L. Sanfilippo[93], D.P.C. Sankey[196], T. Sano[139], A. Sansoni[82], M. Santana Queiroz[20], L. Santi[64], C. Santoni[68], H. Santos[186,187], A. Santra[245], E. Sanzani[30,29], K.A. Saoucha[134], J.G. Saraiva[186,189], J. Sardain[8], O. Sasaki[132], K. Sato[233], C. Sauer[64], E. Sauvan[5], P. Savard[XXXV,230], R. Sawada[228], C. Sawyer[196], L. Sawyer[149], A. M. Sayed[33], C. Sbarra[30], A. Sbrizzi[30,29], T. Scanlon[148], J. Schaarschmidt[207], U. Schäfer[152], A.C. Schaffer[99,73], D. Schaile[161], R.D. Schamberger[218], C. Scharf[21], M.M. Schefer[22], V.A. Schegelsky[65], D. Scheirich[195], M. Schernau[204], C. Scheulen[85], C. Schiavi[87,86], M. Schioppa[72,71], B. Schlag[216], S. Schlenker[64], J. Schmeing[247], E. Schmidt[162], M. A. Schmidt[247], K. Schmieden[31], C. Schmitt[152], N. Schmitt[152], S. Schmitt[77], N.A. Schneider[161], L. Schoeffel[197], A. Schoening[94], P.G. Scholer[57], E. Schopf[214], M. Schott[31], S. Schramm[85], T. Schroer[85], H-C. Schultz-Coulon[93], M. Schumacher[83], B.A. Schumm[198], Ph. Schune[197], H.R. Schwartz[8], A. Schwartzman[216], T.A. Schwarz[158], Ph. Schwemling[197], R. Schwienhorst[159], F.G. Sciacca[22], A. Sciandra[43], G. Sciolla[33], F. Scuri[113], C.D. Sebastiani[64], K. Sedlaczek[170], S.C. Seidel[167], A. Seiden[198], B.D. Seidlitz[69], C. Seitz[77], J.M. Seixas[128], G. Sekhniaidze[109], L. Selem[90], N. Semprini-Cesari[30,29], A. Semushin[249], D. Sengupta[85], V. Senthilkumar[239], L. Serin[99], M. Sessa[109,110], H. Severini[176], F. Sforza[87,86], A. Sfyrla[85], Q. Sha[15], H. Shaddix[170], A.H. Shah[46], R. Shaheen[217], J.D. Shahinian[184], M. Shamim[64], L.Y. Shan[15], M. Shapiro[19], A. Sharma[64], A.S. Sharma[240], P. Sharma[43], P.B. Shatalov[65], K. Shaw[219], S.M. Shaw[153], Q. Shen[15], D.J. Sheppard[215], P. Sherwood[148], L. Shi[148], X. Shi[15], S. Shimizu[132], I.P.J. Shipsey[XLII,182], S. Shirabe[140], M. Shiyakova[XXVI,66], M.J. Shochet[67], D.R. Shope[181], B. Shrestha[176], S. Shrestha[XL,175], I. Shreyber[66], M.J. Shroff[241], P. Sicho[193], A.M. Sickles[238], E. Sideras Haddad[56,236], A. C. Sidley[169], A. Sidoti[30], F. Siegert[79], Dj. Sijacki[17], F. Sili[92], J.M. Silva[81], I. Silva Ferreira[128], M.V. Silva Oliveira[43], S.B. Silverstein[75], S. Simion[99], R. Simoniello[64], E.L. Simpson[153], H. Simpson[219], L.R. Simpson[7], S. Simsek[126], S. Sindhu[84], P. Sinervo[230], S. N. Singh[33], S. Singh[43], S. Sinha[77], S. Sinha[153], M. Sioli[30,29], K. Sioulas[10], I. Siral[64], E. Sitnikova[77], J. Sjölin[75,76], A. Skaf[84], E. Skorda[23], P. Skubic[176], M. Slawinska[138], I. Slazyk[18], I. Sliusar[181], V. Smakhtin[245], B.H. Smart[196], S.Yu. Smirnov[200], Y. Smirnov[126], L.N. Smirnova[I,65], O. Smirnova[150], A.C. Smith[69], D.R. Smith[235], J.L. Smith[153], M. B. Smith[57], R. Smith[216], H. Smitmanns[152], M. Smizanska[143], K. Smolek[194], P. Smolyanskiy[194], A.A. Snesarev[66], H.L. Snoek[169], S. Snyder[43], R. Sobie[XXVIII,241], A. Soffer[226], C.A. Solans Sanchez[64], E.Yu. Soldatov[66], U. Soldevila[239], A.A. Solodkov[56], S. Solomon[33], A. Soloshenko[66], K. Solovieva[83], O.V. Solovyanov[68], P. Sommer[79], A. Sonay[14], A. Sopczak[194], A.L. Sopio[81], F. Sopkova[42], J. D. Sorenson[167], I.R. Sotarriva Alvarez[206], V. Sothilingam[93], O. J. Soto Sandoval[201,200], S. Sottocornola[101], R. Soualah[133], Z. Soumaimi[62], D. South[77], N. Soybelman[245], S. Spagnolo[105,106], M. Spalla[162], D. Sperlich[83], B. Spisso[109,110], D.P. Spiteri[89], L. Splendori[154], M. Spousta[195], E.J. Staats[57], R. Stamen[93], E. Stanecka[138], W. Stanek-Maslouska[77], M.V. Stange[79], B. Stanislaus[19], M.M. Stanitzki[77], E.A. Starchenko[65], G.H. Stark[198], J. Stark[141], P. Staroba[193], P. Starovoitov[134], R. Staszewski[138], C. Stauch[161], G. Stavropoulos[74], A. Stefl[64], A. Stein[152], P. Steinberg[43], B. Stelzer[215,231], H.J. Stelzer[185], O. Stelzer[231], H. Stenzel[88], T.J. Stevenson[219], G.A. Stewart[64], J.R. Stewart[177], G. Stoicea[35], M. Stolarski[186], S. Stonjek[162], A. Straessner[79], J. Strandberg[217], S. Strandberg[75,76], M. Stratmann[247], M. Strauss[176], T. Strebler[154], P. Strizenec[42], R. Ströhmer[242], D.M. Strom[179], R. Stroynowski[73], A. Strubig[75,76], S.A. Stucci[43], B. Stugu[18], J. Stupak[176], N.A. Styles[77], D. Su[216], S. Su[92], X. Su[92], D. Suchy[41], A. D. Sudhakar Ponnu[84], K. Sugizaki[184], V.V. Sulin[65], D.M.S. Sultan[182], L. Sultanaliyeva[31], S. Sultansoy[4], S. Sun[246], W. Sun[15], N. Sur[150], M.R. Sutton[219], M. Svatos[193], P. N. Swallow[46], M. Swiatlowski[231], A. Swoboda[64], I. Sykora[41], M. Sykora[195], T. Sykora[195], D. Ta[152], K. Tackmann[XXV,77], A. Taffard[235], R. Tafirout[231], Y. Takubo[132], M. Talby[154], A.A. Talyshev[65], K.C. Tam[96], N.M. Tamir[226], A. Tanaka[228], J. Tanaka[228], R. Tanaka[99], M. Tanasini[218], Z. Tao[240], S. Tapia Araya[205], S. Tapprogge[152], A. Tarek Abouelfadl Mohamed[64], S. Tarem[225], K. Tariq[15], G. Tarna[64], G.F. Tartarelli[107], M. J. Tartarin[141], P. Tas[195], M. Tasevsky[193], E. Tassi[72,71], A.C. Tate[238], Y. Tayalati[XXVII,62], G.N. Taylor[157], W. Taylor[232], R.J. Taylor Vara[239], A.S. Tegetmeier[141], P. Teixeira-Dias[147], J.J. Teoh[230], K. Terashi[228], J. Terron[151], S. Terzo[14], M. Testa[82], R.J. Teuscher[XXVIII,230], A. Thaler[123], O. Theiner[85], T. Theveneaux-Pelzer[154], D.W. Thomas[147], J.P. Thomas[23], E.A. Thompson[19], P.D. Thompson[23], E. Thomson[184], R. E. Thornberry[73], C. Tian[92], Y. Tian[85], V. Tikhomirov[126], Yu.A. Tikhonov[66], S. Timoshenko[65], D. Timoshyn[195], E.X.L. Ting[1], P. Tipton[248], A. Tishelman-Charny[43], K. Todome[206], S. Todorova-Nova[195], L. Toffolin[102,104], M. Togawa[132], J. Tojo[140], S. Tokár[41], O. Toldaiev[101], G. Tolkachev[154], M. Tomoto[132], L. Tompkins[XIV,216], E. Torrence[179], H. Torres[141], D. I. Torres Arza[205], E. Torró Pastor[239], M. Toscani[44], C. Tosciri[67], M. Tost[12], D.R. Tovey[212], T. Trefzger[242], P.M. Tricarico[14], A. Tricoli[43], I.M. Trigger[231], S. Trincaz-Duvoid[183], D.A. Trischuk[241], A. Tropina[66], D. Truncali[117,118], L. Truong[49], M. Trzebinski[138], A. Trzupek[138], F. Tsai[218], M. Tsai[158], A. Tsiamis[227], P.V. Tsiareshka[66], S. Tsigaridas[231], A. Tsirigotis[XXI,227], V. Tsiskaridze[222], E.G. Tskhadadze[222], Y. Tsujikawa[139], I.I. Tsukerman[65], V. Tsulaia[19], S. Tsuno[132], K. Tsuri[174], D. Tsybychev[218], Y. Tu[96], A. Tudorache[35], V. Tudorache[35], S. B. Tuncay[182], S. Turchikhin[87,86], I. Turk Cakir[3], R. Turra[107], T. Turtuvshin[XXIX,66], P.M. Tuts[69], S. Tzamarias[IV,227], Y. Uematsu[132], F. Ukegawa[233], P.A. Ulloa Poblete[201,200], E.N. Umaka[43], G. Unal[64], A. Undrus[43], G. Unel[235], J. Urban[42], P. Urrejola[203], G. Usai[9], R. Ushioda[229], M. Usman[160], F. Ustuner[81], Z. Uysal[126], V. Vacek[194], B. Vachon[156], T. Vafeiadis[64], A. Vaitkus[148], C. Valderanis[161], E. Valdes Santurio[75,76], M. Valente[64], S. Valentinetti[30,29], A. Valero[239], E. Valiente Moreno[239], A. Vallier[141], J.A. Valls Ferrer[239], D. R. Van Arneman[169], A. Van Der Graaf[78], H. Z. Van Der Schyf[56], P. Van Gemmeren[7], M. Van Rijnbach[64], S. Van Stroud[148], I. Van Vulpen[169], P. Vana[195], M. Vanadia[117,118], U. M. Vande Voorde[217], W. Vandelli[64], E.R. Vandewall[216], D. Vannicola[226], L. Vannoli[82], R. Vari[115], M. Varma[248], E.W. Varnes[8], C. Varni[170], D. Varouchas[99], L. Varriale[239], K.E. Varvell[220], M.E. Vasile[35], L. Vaslin[132], M. D. Vassilev[216], A. Vasyukov[66], L. M. Vaughan[177], R. Vavricka[195], T. Vazquez Schroeder[14], J. Veatch[45], V. Vecchio[153], M.J. Veen[155], I. Veliscek[43], I. Velkovska[145], L.M. Veloce[230], F. Veloso[186,188], A.G. Veltman[81], S. Veneziano[115], A. Ventura[105,106], A. Verbytskyi[162], M. Verducci[113,114], C. Vergis[146], M. Verissimo De Araujo[128], W. Verkerke[169], J.C. Vermeulen[169], C. Vernieri[216], M. Vessella[235], M.C. Vetterli[XXXV,215], A. Vgenopoulos[152], N. Viaux Maira[XXXII,205], T. Vickey[212], O.E. Vickey Boeriu[212], G.H.A. Viehhauser[182], L. Vigani[94], M. Vigl[162], M. Villa[30,29], M. Villaplana Perez[239], E.M. Villhauer[67], E. Vilucchi[82], M. Vincent[239], M.G. Vincter[57], A. Visibile[169], A. Visive[169], C. Vittori[64], I. Vivarelli[30,29], M.I. Vi-

vas Albornoz[77], E. Voevodina[162], F. Vogel[161], J.C. Voigt[79], P. Vokac[194], Yu. Volkotrub[137], L. Vomberg[31], E. Von Toerne[31], B. Vormwald[64], K. Vorobev[80], M. Vos[239], K. Voss[214], M. Vozak[64], L. Vozdecky[176], N. Vranjes[17], M. Vranjes Milosavljevic[17], M. Vreeswijk[169], N.K. Vu[211,210], R. Vuillermet[64], O. Vujinovic[152], I. Vukotic[67], I. K. Vyas[57], J.F. Wack[46], S. Wada[233], C. Wagner[216], J.M. Wagner[19], W. Wagner[247], S. Wahdan[247], H. Wahlberg[142], C. H. Waits[176], J. Walder[196], R. Walker[161], K. Walkingshaw Pass[89], W. Walkowiak[214], A. Wall[184], E.J. Wallin[150], T. Wamorkar[19], K. Wandall-Christensen[239], A. Wang[92], A.Z. Wang[198], C. Wang[152], C. Wang[12], H. Wang[19], J. Wang[97], P. Wang[153], P. Wang[148], R. Wang[91], R. Wang[7], S.M. Wang[221], S. Wang[15], T. Wang[168], T. Wang[92], W.T. Wang[182], W. Wang[15], X. Wang[238], X. Wang[210], X. Wang[77], Y. Wang[218], Y. Wang[92], Z. Wang[158], Z. Wang[211], Z. Wang[158], C. Wanotayaroj[132], A. Warburton[156], A.L. Warnerbring[214], S. Waterhouse[147], A.T. Watson[23], H. Watson[81], M.F. Watson[23], E. Watton[64], G. Watts[207], B.M. Waugh[148], J. M. Webb[83], C. Weber[43], H. A. Weber[21], M.S. Weber[22], S.M. Weber[93], C. Wei[92], Y. Wei[83], A.R. Weidberg[182], E.J. Weik[173], J. Weingarten[78], C. Weiser[83], C.J. Wells[77], T. Wenaus[43], T. Wengler[64], N.S. Wenke[162], N. Wermes[31], M. Wessels[93], A.M. Wharton[143], A.S. White[91], A. White[9], M.J. White[1], D. Whiteson[235], L. Wickremasinghe[180], W. Wiedenmann[246], M. Wielers[196], R. Wierda[217], C. Wiglesworth[70], D.J. Wilbern[176], H.G. Wilkens[64], J. J. H. Wilkinson[46], D.M. Williams[69], H.H. Williams[184], S. Williams[46], S. Willocq[155], B.J. Wilson[153], D.J. Wilson[153], P.J. Windischhofer[67], F.I. Winkel[44], F. Winklmeier[179], B.T. Winter[83], M. Wittgen[216], M. Wobisch[149], T. Wojtkowski[90], Z. Wolffs[169], J. Wollrath[64], M.W. Wolter[138], H. Wolters[186,188], M.C. Wong[198], E.L. Woodward[69], S.D. Worm[77], B.K. Wosiek[138], K.W. Woźniak[138], S. Wozniewski[84], K. Wraight[89], C. Wu[230], C. Wu[23], J. Wu[228], M. Wu[165], M. Wu[168], S.L. Wu[246], S. Wu[XXXVII,15], X. Wu[92], Y.Q. Wu[230], Y. Wu[92], Z. Wu[5], Z. Wu[164], J. Wuerzinger[162], T.R. Wyatt[153], B.M. Wynne[81], S. Xella[70], L. Xia[164], M. Xie[92], A. Xiong[179], D. Xu[15], H. Xu[92], L. Xu[92], R. Xu[184], T. Xu[158], Y. Xu[207], Z. Xu[81], R. Xue[185], B. Yabsley[220], S. Yacoob[47], Y. Yamaguchi[132], E. Yamashita[228], H. Yamauchi[233], T. Yamazaki[19], Y. Yamazaki[135], S. Yan[89], Z. Yan[155], H.J. Yang[210,211], H.T. Yang[92], S. Yang[92], T. Yang[97], X. Yang[64], X. Yang[15], Y. Yang[228], Y. Yang[92], W-M. Yao[19], C. L. Yardley[219], J. Ye[15], S. Ye[43], X. Ye[92], Y. Yeh[148], I. Yeletskikh[66], B. Yeo[20], M.R. Yexley[148], T. P. Yildirim[182], K. Yorita[244], C.J.S. Young[64], C. Young[216], N.D. Young[179], Y. Yu[92], J. Yuan[15,166], M. Yuan[158], R. Yuan[211], L. Yue[148], M. Zaazoua[92], B. Zabinski[138], I. Zahir[58], A. Zaio[87,86], Z.K. Zak[138], T. Zakareishvili[239], S. Zambito[85], J.A. Zamora Saa[202], J. Zang[228], R. Zanzottera[107,108], O. Zaplatilek[194], C. Zeitnitz[247], H. Zeng[15], D.T. Zenger Jr[33], O. Zenin[65], T. Ženiš[41], S. Zenz[146], D. Zerwas[99], M. Zhai[15,166], D.F. Zhang[212], G. Zhang[XXXVII,15], J. Zhang[208], J. Zhang[7], L. Zhang[92], L. Zhang[164], P. Zhang[15,166], R. Zhang[164], S. Zhang[141], T. Zhang[228], Y. Zhang[207], Y. Zhang[148], Y. Zhang[92], Y. Zhang[164], Z. Zhang[19], Z. Zhang[208], Z. Zhang[99], H. Zhao[207], T. Zhao[208], Y. Zhao[57], Z. Zhao[92], Z. Zhao[92], A. Zhemchugov[66], J. Zheng[164], K. Zheng[238], X. Zheng[92], Z. Zheng[216], D. Zhong[238], B. Zhou[158], H. Zhou[8], N. Zhou[210], Y. Zhou[16], Y. Zhou[164], Y. Zhou[8], J. Zhu[158], X. Zhu[211], Y. Zhu[210], Y. Zhu[92], X. Zhuang[15], K. Zhukov[101], N.I. Zimine[66], J. Zinsser[94], M. Ziolkowski[214], L. Živković[17], A. Zoccoli[30,29], K. Zoch[91], A. Zografos[64], T.G. Zorbas[212], O. Zormpa[74], L. Zwalinski[64]

Affiliation Notes

[I] Affiliated with an institute formerly covered by a cooperation agreement with CERN
[II] An-Najah National University, Nablus, Palestine
[III] Borough of Manhattan Community College, City University of New York, New York NY, United States of America
[IV] Center for Interdisciplinary Research and Innovation (CIRI-AUTH), Thessaloniki, Greece
[V] Centre of Physics of the Universities of Minho and Porto (CF-UM-UP), Portugal
[VI] CERN, Geneva, Switzerland
[VII] Département de Physique Nucléaire et Corpusculaire, Université de Genève, Genève, Switzerland
[VIII] Departament de Fisica de la Universitat Autonoma de Barcelona, Barcelona, Spain
[IX] Department of Financial and Management Engineering, University of the Aegean, Chios, Greece
[X] Department of Mathematical Sciences, University of South Africa, Johannesburg, South Africa
[XI] Department of Modern Physics and State Key Laboratory of Particle Detection and Electronics, University of Science and Technology of China, Hefei, China
[XII] Department of Physics, Bolu Abant Izzet Baysal University, Bolu, Türkiye
[XIII] Department of Physics, King's College London, London, United Kingdom
[XIV] Department of Physics, Stanford University, Stanford CA, United States of America
[XV] Department of Physics, Stellenbosch University, South Africa
[XVI] Department of Physics, University of Fribourg, Fribourg, Switzerland
[XVII] Department of Physics, University of Thessaly, Greece
[XVIII] Department of Physics, Westmont College, Santa Barbara, United States of America
[XIX] Faculty of Physics, Sofia University, 'St. Kliment Ohridski', Sofia, Bulgaria
[XX] Faculty of Physics, University of Bucharest, Romania
[XXI] Hellenic Open University, Patras, Greece
[XXII] Henan University, China
[XXIII] Imam Mohammad Ibn Saud Islamic University, Saudi Arabia
[XXIV] Institucio Catalana de Recerca i Estudis Avancats, ICREA, Barcelona, Spain
[XXV] Institut für Experimentalphysik, Universität Hamburg, Hamburg, Germany
[XXVI] Institute for Nuclear Research and Nuclear Energy (INRNE) of the Bulgarian Academy of Sciences, Sofia, Bulgaria
[XXVII] Institute of Applied Physics, Mohammed VI Polytechnic University, Ben Guerir, Morocco
[XXVIII] Institute of Particle Physics (IPP), Canada
[XXIX] Institute of Physics and Technology, Mongolian Academy of Sciences, Ulaanbaatar, Mongolia
[XXX] Institute of Physics, Azerbaijan Academy of Sciences, Baku, Azerbaijan
[XXXI] Institute of Theoretical Physics, Ilia State University, Tbilisi, Georgia
[XXXII] Millennium Institute for Subatomic physics at high energy frontier (SAPHIR), Santiago, Chile
[XXXIII] National Institute of Physics, University of the Philippines Diliman (Philippines), Philippines
[XXXIV] The Collaborative Innovation Center of Quantum Matter (CICQM), Beijing, China
[XXXV] TRIUMF, Vancouver BC, Canada
[XXXVI] Università di Napoli Parthenope, Napoli, Italy
[XXXVII] University of Chinese Academy of Sciences (UCAS), Beijing, China
[XXXVIII] University of Colorado Boulder, Department of Physics, Colorado, United States of America
[XXXIX] University of Siena, Italy
[XL] Washington College, Chestertown, MD, United States of America
[XLI] Yeditepe University, Physics Department, Istanbul, Türkiye
[XLII] Deceased

Collaboration Institutes

[1] Department of Physics, University of Adelaide, Adelaide, Australia
[2] Department of Physics, University of Alberta, Edmonton AB, Canada
[3] Department of Physics, Ankara University, Ankara, Türkiye
[4] Division of Physics, TOBB University of Economics and Technology, Ankara, Türkiye
[5] LAPP, Université Savoie Mont Blanc, CNRS/IN2P3, Annecy, France
[6] APC, Université Paris Cité, CNRS/IN2P3, Paris, France
[7] High Energy Physics Division, Argonne National Laboratory, Argonne IL, United States of America
[8] Department of Physics, University of Arizona, Tucson AZ, United States of America
[9] Department of Physics, University of Texas at Arlington, Arlington TX, United States of America
[10] Physics Department, National and Kapodistrian University of Athens, Athens, Greece
[11] Physics Department, National Technical University of Athens, Zografou, Greece
[12] Department of Physics, University of Texas at Austin, Austin TX, United States of America
[13] Institute of Physics, Azerbaijan Academy of Sciences, Baku, Azerbaijan
[14] Institut de Física d'Altes Energies (IFAE), Barcelona Institute of Science and Technology, Barcelona, Spain
[15] Institute of High Energy Physics, Chinese Academy of Sciences, Beijing, China
[16] Physics Department, Tsinghua University, Beijing, China
[17] Institute of Physics, University of Belgrade, Belgrade, Serbia
[18] Department for Physics and Technology, University of Bergen, Bergen, Norway
[19] Physics Division, Lawrence Berkeley National Laboratory, Berkeley CA, United States of America
[20] University of California, Berkeley CA, United States of America
[21] Institut für Physik, Humboldt Universität zu Berlin, Berlin, Germany
[22] Albert Einstein Center for Fundamental Physics and Laboratory for High Energy Physics, University of Bern, Bern, Switzerland
[23] School of Physics and Astronomy, University of Birmingham, Birmingham, United Kingdom
[24] Department of Physics, Bogazici University, Istanbul, Türkiye
[25] Department of Physics Engineering, Gaziantep University, Gaziantep, Türkiye
[26] Department of Physics, Istanbul University, Istanbul, Türkiye
[27] Facultad de Ciencias y Centro de Investigaciónes, Universidad Antonio Nariño, Bogotá, Colombia
[28] Departamento de Física, Universidad Nacional de Colombia, Bogotá, Colombia
[29] Dipartimento di Fisica e Astronomia A. Righi, Università di Bologna, Bologna, Italy
[30] INFN Sezione di Bologna, Italy
[31] Physikalisches Institut, Universität Bonn, Bonn, Germany
[32] Department of Physics, Boston University, Boston MA, United States of America
[33] Department of Physics, Brandeis University, Waltham MA, United States of America
[34] Transilvania University of Brasov, Brasov, Romania
[35] Horia Hulubei National Institute of Physics and Nuclear Engineering, Bucharest, Romania
[36] Department of Physics, Alexandru Ioan Cuza University of Iasi, Iasi, Romania
[37] National Institute for Research and Development of Isotopic and Molecular Technologies, Physics Department, Cluj-Napoca, Romania
[38] National University of Science and Technology Politechnica, Bucharest, Romania
[39] West University in Timisoara, Timisoara, Romania
[40] Faculty of Physics, University of Bucharest, Bucharest, Romania
[41] Faculty of Mathematics, Physics and Informatics, Comenius University, Bratislava, Slovak Republic
[42] Department of Subnuclear Physics, Institute of Experimental Physics of the Slovak Academy of Sciences, Kosice, Slovak Republic
[43] Physics Department, Brookhaven National Laboratory, Upton NY, United States of America
[44] Universidad de Buenos Aires, Facultad de Ciencias Exactas y Naturales, Departamento de Física, y CONICET, Instituto de Física de Buenos Aires (IFIBA), Buenos Aires, Argentina
[45] California State University, CA, United States of America
[46] Cavendish Laboratory, University of Cambridge, Cambridge, United Kingdom
[47] Department of Physics, University of Cape Town, Cape Town, South Africa
[48] iThemba Labs, Western Cape, South Africa
[49] Department of Mechanical Engineering Science, University of Johannesburg, Johannesburg, South Africa
[50] National Institute of Physics, University of the Philippines Diliman (Philippines), Philippines
[51] Department of Physics, Stellenbosch University, Matieland, South Africa
[52] University of KwaZulu-Natal, School of Agriculture and Science, Mathematics, Westville, South Africa
[53] University of South Africa, Department of Physics, Pretoria, South Africa
[54] University of Pretoria, Department of Mechanical and Aeronautical Engineering, Pretoria, South Africa
[55] University of Zululand, KwaDlangezwa, South Africa
[56] School of Physics, University of the Witwatersrand, Johannesburg, South Africa
[57] Department of Physics, Carleton University, Ottawa ON, Canada
[58] Faculté des Sciences Ain Chock, Université Hassan II de Casablanca, Morocco
[59] Faculté des Sciences, Université Ibn-Tofail, Kénitra, Morocco
[60] Faculté des Sciences Semlalia, Université Cadi Ayyad, LPHEA-Marrakech, Morocco
[61] LPMR, Faculté des Sciences, Université Mohamed Premier, Oujda, Morocco
[62] Faculté des sciences, Université Mohammed V, Rabat, Morocco
[63] Institute of Applied Physics, Mohammed VI Polytechnic University, Ben Guerir, Morocco
[64] CERN, Geneva, Switzerland
[65] Affiliated with an institute formerly covered by a cooperation agreement with CERN
[66] Affiliated with an international laboratory covered by a cooperation agreement with CERN
[67] Enrico Fermi Institute, University of Chicago, Chicago IL, United States of America
[68] LPC, Université Clermont Auvergne, CNRS/IN2P3, Clermont-Ferrand, France
[69] Nevis Laboratory, Columbia University, Irvington NY, United States of America
[70] Niels Bohr Institute, University of Copenhagen, Copenhagen, Denmark
[71] Dipartimento di Fisica, Università della Calabria, Rende, Italy
[72] INFN Gruppo Collegato di Cosenza, Laboratori Nazionali di Frascati, Italy
[73] Physics Department, Southern Methodist University, Dallas TX, United States of America
[74] National Centre for Scientific Research "Demokritos", Agia Paraskevi, Greece
[75] Department of Physics, Stockholm University, Sweden
[76] Oskar Klein Centre, Stockholm, Sweden
[77] Deutsches Elektronen-Synchrotron DESY, Hamburg and Zeuthen, Germany

[78] Fakultät Physik, Technische Universität Dortmund, Dortmund, Germany
[79] Institut für Kern- und Teilchenphysik, Technische Universität Dresden, Dresden, Germany
[80] Department of Physics, Duke University, Durham NC, United States of America
[81] SUPA - School of Physics and Astronomy, University of Edinburgh, Edinburgh, United Kingdom
[82] INFN e Laboratori Nazionali di Frascati, Frascati, Italy
[83] Physikalisches Institut, Albert-Ludwigs-Universität Freiburg, Freiburg, Germany
[84] II. Physikalisches Institut, Georg-August-Universität Göttingen, Göttingen, Germany
[85] Département de Physique Nucléaire et Corpusculaire, Université de Genève, Genève, Switzerland
[86] Dipartimento di Fisica, Università di Genova, Genova, Italy
[87] INFN Sezione di Genova, Italy
[88] II. Physikalisches Institut, Justus-Liebig-Universität Giessen, Giessen, Germany
[89] SUPA - School of Physics and Astronomy, University of Glasgow, Glasgow, United Kingdom
[90] LPSC, Université Grenoble Alpes, CNRS/IN2P3, Grenoble INP, Grenoble, France
[91] Laboratory for Particle Physics and Cosmology, Harvard University, Cambridge MA, United States of America
[92] Department of Modern Physics and State Key Laboratory of Particle Detection and Electronics, University of Science and Technology of China, Hefei, China
[93] Kirchhoff-Institut für Physik, Ruprecht-Karls-Universität Heidelberg, Heidelberg, Germany
[94] Physikalisches Institut, Ruprecht-Karls-Universität Heidelberg, Heidelberg, Germany
[95] Department of Physics, Chinese University of Hong Kong, Shatin, N.T., Hong Kong, China
[96] Department of Physics, University of Hong Kong, Hong Kong, China
[97] Department of Physics and Institute for Advanced Study, Hong Kong University of Science and Technology, Clear Water Bay, Kowloon, Hong Kong, China
[98] Department of Physics, National Tsing Hua University, Hsinchu, Taiwan
[99] IJCLab, Université Paris-Saclay, CNRS/IN2P3, 91405, Orsay, France
[100] Centro Nacional de Microelectrónica (IMB-CNM-CSIC), Barcelona, Spain
[101] Department of Physics, Indiana University, Bloomington IN, United States of America
[102] INFN Gruppo Collegato di Udine, Sezione di Trieste, Udine, Italy
[103] ICTP, Trieste, Italy
[104] Dipartimento Politecnico di Ingegneria e Architettura, Università di Udine, Udine, Italy
[105] INFN Sezione di Lecce, Italy
[106] Dipartimento di Matematica e Fisica, Università del Salento, Lecce, Italy
[107] INFN Sezione di Milano, Italy
[108] Dipartimento di Fisica, Università di Milano, Milano, Italy
[109] INFN Sezione di Napoli, Italy
[110] Dipartimento di Fisica, Università di Napoli, Napoli, Italy
[111] INFN Sezione di Pavia, Italy
[112] Dipartimento di Fisica, Università di Pavia, Pavia, Italy
[113] INFN Sezione di Pisa, Italy
[114] Dipartimento di Fisica E. Fermi, Università di Pisa, Pisa, Italy
[115] INFN Sezione di Roma, Italy
[116] Dipartimento di Fisica, Sapienza Università di Roma, Roma, Italy
[117] INFN Sezione di Roma Tor Vergata, Italy
[118] Dipartimento di Fisica, Università di Roma Tor Vergata, Roma, Italy
[119] INFN Sezione di Roma Tre, Italy
[120] Dipartimento di Matematica e Fisica, Università Roma Tre, Roma, Italy
[121] INFN-TIFPA, Italy
[122] Università degli Studi di Trento, Trento, Italy
[123] Universität Innsbruck, Department of Astro and Particle Physics, Innsbruck, Austria
[124] University of Iowa, Iowa City IA, United States of America
[125] Department of Physics and Astronomy, Iowa State University, Ames IA, United States of America
[126] Istinye University, Sariyer, Istanbul, Türkiye
[127] Departamento de Engenharia Elétrica, Universidade Federal de Juiz de Fora (UFJF), Juiz de Fora, Brazil
[128] Universidade Federal do Rio De Janeiro COPPE/EE/IF, Rio de Janeiro, Brazil
[129] Instituto de Física, Universidade de São Paulo, São Paulo, Brazil
[130] Rio de Janeiro State University, Rio de Janeiro, Brazil
[131] Federal University of Bahia, Bahia, Brazil
[132] KEK, High Energy Accelerator Research Organization, Tsukuba, Japan
[133] Khalifa University of Science and Technology, Abu Dhabi, United Arab Emirates
[134] University of Sharjah, Sharjah, United Arab Emirates
[135] Graduate School of Science, Kobe University, Kobe, Japan
[136] AGH University of Krakow, Faculty of Physics and Applied Computer Science, Krakow, Poland
[137] Marian Smoluchowski Institute of Physics, Jagiellonian University, Krakow, Poland
[138] Institute of Nuclear Physics Polish Academy of Sciences, Krakow, Poland
[139] Faculty of Science, Kyoto University, Kyoto, Japan
[140] Research Center for Advanced Particle Physics and Department of Physics, Kyushu University, Fukuoka , Japan
[141] L2IT, Université de Toulouse, CNRS/IN2P3, UPS, Toulouse, France
[142] Instituto de Física La Plata, Universidad Nacional de La Plata and CONICET, La Plata, Argentina
[143] Physics Department, Lancaster University, Lancaster, United Kingdom
[144] Oliver Lodge Laboratory, University of Liverpool, Liverpool, United Kingdom
[145] Department of Experimental Particle Physics, Jožef Stefan Institute and Department of Physics, University of Ljubljana, Ljubljana, Slovenia
[146] Department of Physics and Astronomy, Queen Mary University of London, London, United Kingdom
[147] Department of Physics, Royal Holloway University of London, Egham, United Kingdom
[148] Department of Physics and Astronomy, University College London, London, United Kingdom
[149] Louisiana Tech University, Ruston LA, United States of America
[150] Fysiska institutionen, Lunds universitet, Lund, Sweden
[151] Departamento de Física Teorica C-15 and CIAFF, Universidad Autónoma de Madrid, Madrid, Spain
[152] Institut für Physik, Universität Mainz, Mainz, Germany
[153] School of Physics and Astronomy, University of Manchester, Manchester, United Kingdom
[154] CPPM, Aix-Marseille Université, CNRS/IN2P3, Marseille, France
[155] Department of Physics, University of Massachusetts, Amherst MA, United States of America
[156] Department of Physics, McGill University, Montreal QC, Canada
[157] School of Physics, University of Melbourne, Victoria, Australia
[158] Department of Physics, University of Michigan, Ann Arbor MI, United States of America
[159] Department of Physics and Astronomy, Michigan State University, East Lansing MI, United States of America
[160] Group of Particle Physics, University of Montreal, Montreal QC, Canada

[161] Fakultät für Physik, Ludwig-Maximilians-Universität München, München, Germany
[162] Max-Planck-Institut für Physik (Werner-Heisenberg-Institut), München, Germany
[163] Graduate School of Science and Kobayashi-Maskawa Institute, Nagoya University, Nagoya, Japan
[164] Department of Physics, Nanjing University, Nanjing, China
[165] School of Science, Shenzhen Campus of Sun Yat-sen University, China
[166] University of Chinese Academy of Science (UCAS), Beijing, China
[167] Department of Physics and Astronomy, University of New Mexico, Albuquerque NM, United States of America
[168] Institute for Mathematics, Astrophysics and Particle Physics, Radboud University/Nikhef, Nijmegen, Netherlands
[169] Nikhef National Institute for Subatomic Physics and University of Amsterdam, Amsterdam, Netherlands
[170] Department of Physics, Northern Illinois University, DeKalb IL, United States of America
[171] New York University Abu Dhabi, Abu Dhabi, United Arab Emirates
[172] United Arab Emirates University, Al Ain, United Arab Emirates
[173] Department of Physics, New York University, New York NY, United States of America
[174] Ochanomizu University, Otsuka, Bunkyo-ku, Tokyo, Japan
[175] Ohio State University, Columbus OH, United States of America
[176] Homer L. Dodge Department of Physics and Astronomy, University of Oklahoma, Norman OK, United States of America
[177] Department of Physics, Oklahoma State University, Stillwater OK, United States of America
[178] Palacký University, Joint Laboratory of Optics, Olomouc, Czech Republic
[179] Institute for Fundamental Science, University of Oregon, Eugene, OR, United States of America
[180] Graduate School of Science, University of Osaka, Osaka, Japan
[181] Department of Physics, University of Oslo, Oslo, Norway
[182] Department of Physics, Oxford University, Oxford, United Kingdom
[183] LPNHE, Sorbonne Université, Université Paris Cité, CNRS/IN2P3, Paris, France
[184] Department of Physics, University of Pennsylvania, Philadelphia PA, United States of America
[185] Department of Physics and Astronomy, University of Pittsburgh, Pittsburgh PA, United States of America
[186] Laboratório de Instrumentação e Física Experimental de Partículas - LIP, Lisboa, Portugal
[187] Departamento de Física, Faculdade de Ciências, Universidade de Lisboa, Lisboa, Portugal
[188] Departamento de Física, Universidade de Coimbra, Coimbra, Portugal
[189] Centro de Física Nuclear da Universidade de Lisboa, Lisboa, Portugal
[190] Departamento de Física, Escola de Ciências, Universidade do Minho, Braga, Portugal
[191] Departamento de Física Teórica y del Cosmos, Universidad de Granada, Granada (Spain), Spain
[192] Departamento de Física, Instituto Superior Técnico, Universidade de Lisboa, Lisboa, Portugal
[193] Institute of Physics of the Czech Academy of Sciences, Prague, Czech Republic
[194] Czech Technical University in Prague, Prague, Czech Republic
[195] Charles University, Faculty of Mathematics and Physics, Prague, Czech Republic
[196] Particle Physics Department, Rutherford Appleton Laboratory, Didcot, United Kingdom
[197] IRFU, CEA, Université Paris-Saclay, Gif-sur-Yvette, France
[198] Santa Cruz Institute for Particle Physics, University of California Santa Cruz, Santa Cruz CA, United States of America
[199] Departamento de Física, Pontificia Universidad Católica de Chile, Santiago, Chile
[200] Millennium Institute for Subatomic physics at high energy frontier (SAPHIR), Santiago, Chile
[201] Instituto de Investigación Multidisciplinario en Ciencia y Tecnología, y Departamento de Física, Universidad de La Serena, Chile
[202] Universidad Andres Bello, Department of Physics, Santiago, Chile
[203] Universidad San Sebastian, Recoleta, Chile
[204] Instituto de Alta Investigación, Universidad de Tarapacá, Arica, Chile
[205] Departamento de Física, Universidad Técnica Federico Santa María, Valparaíso, Chile
[206] Department of Physics, Institute of Science, Tokyo, Japan
[207] Department of Physics, University of Washington, Seattle WA, United States of America
[208] Institute of Frontier and Interdisciplinary Science and Key Laboratory of Particle Physics and Particle Irradiation (MOE), Shandong University, Qingdao, China
[209] School of Physics, Zhengzhou University, China
[210] State Key Laboratory of Dark Matter Physics, School of Physics and Astronomy, Shanghai Jiao Tong University, Key Laboratory for Particle Astrophysics and Cosmology (MOE), SKLPPC, Shanghai, China
[211] State Key Laboratory of Dark Matter Physics, Tsung-Dao Lee Institute, Shanghai Jiao Tong University, Shanghai, China
[212] Department of Physics and Astronomy, University of Sheffield, Sheffield, United Kingdom
[213] Department of Physics, Shinshu University, Nagano, Japan
[214] Department Physik, Universität Siegen, Siegen, Germany
[215] Department of Physics, Simon Fraser University, Burnaby BC, Canada
[216] SLAC National Accelerator Laboratory, Stanford CA, United States of America
[217] Department of Physics, Royal Institute of Technology, Stockholm, Sweden
[218] Departments of Physics and Astronomy, Stony Brook University, Stony Brook NY, United States of America
[219] Department of Physics and Astronomy, University of Sussex, Brighton, United Kingdom
[220] School of Physics, University of Sydney, Sydney, Australia
[221] Institute of Physics, Academia Sinica, Taipei, Taiwan
[222] E. Andronikashvili Institute of Physics, Iv. Javakhishvili Tbilisi State University, Tbilisi, Georgia
[223] High Energy Physics Institute, Tbilisi State University, Tbilisi, Georgia
[224] University of Georgia, Tbilisi, Georgia
[225] Department of Physics, Technion, Israel Institute of Technology, Haifa, Israel
[226] Raymond and Beverly Sackler School of Physics and Astronomy, Tel Aviv University, Tel Aviv, Israel
[227] Department of Physics, Aristotle University of Thessaloniki, Thessaloniki, Greece
[228] International Center for Elementary Particle Physics and Department of Physics, University of Tokyo, Tokyo, Japan
[229] Graduate School of Science and Technology, Tokyo Metropolitan University, Tokyo, Japan
[230] Department of Physics, University of Toronto, Toronto ON, Canada
[231] TRIUMF, Vancouver BC, Canada
[232] Department of Physics and Astronomy, York University, Toronto ON, Canada
[233] Division of Physics and Tomonaga Center for the History of the Universe, Faculty of Pure and Applied Sciences, University of Tsukuba, Tsukuba, Japan
[234] Department of Physics and Astronomy, Tufts University, Medford MA, United States of America
[235] Department of Physics and Astronomy, University of California Irvine, Irvine CA, United States of America
[236] University of West Attica, Athens, Greece
[237] Department of Physics and Astronomy, University of Uppsala, Uppsala, Sweden

[238] Department of Physics, University of Illinois, Urbana IL, United States of America
[239] Instituto de Física Corpuscular (IFIC), Centro Mixto Universidad de Valencia - CSIC, Valencia, Spain
[240] Department of Physics, University of British Columbia, Vancouver BC, Canada
[241] Department of Physics and Astronomy, University of Victoria, Victoria BC, Canada
[242] Fakultät für Physik und Astronomie, Julius-Maximilians-Universität Würzburg, Würzburg, Germany
[243] Department of Physics, University of Warwick, Coventry, United Kingdom
[244] Waseda University, Tokyo, Japan
[245] Department of Particle Physics and Astrophysics, Weizmann Institute of Science, Rehovot, Israel
[246] Department of Physics, University of Wisconsin, Madison WI, United States of America
[247] Fakultät für Mathematik und Naturwissenschaften, Fachgruppe Physik, Bergische Universität Wuppertal, Wuppertal, Germany
[248] Department of Physics, Yale University, New Haven CT, United States of America
[249] Yerevan Physics Institute, Yerevan, Armenia

References

[1] S. Godfrey, Quartic gauge boson couplings, AIP Conf. Proc. 350 (1995) 209–223. hep-ph/9505252 https://doi.org/10.1063/1.49305
[2] ATLAS Collaboration, The ATLAS experiment at the CERN large hadron collider, JINST 3 (2008) S08003. https://doi.org/10.1088/1748-0221/3/08/S08003
[3] CMS Collaboration, The CMS experiment at the CERN LHC, JINST 3 (2008) S08004. https://doi.org/10.1088/1748-0221/3/08/S08004
[4] O.S. BrÃ¼ning, et al., LHC Design Report, CERN Yellow Reports: Monographs, CERN, Geneva, 2004. https://doi.org/10.5170/CERN-2004-003-V-1
[5] ATLAS Collaboration, Study of $WW\gamma$ and $WZ\gamma$ production in pp collisions at $\sqrt{s} = 8$ TeV and search for anomalous quartic gauge couplings with the ATLAS experiment, Eur. Phys. J. C 77 (2017) 646. 1707.05597 https://doi.org/10.1140/epjc/s10052-017-5180-3
[6] CMS Collaboration, Search for $WW\gamma$ and $WZ\gamma$ production and constraints on anomalous quartic gauge couplings in pp collisions at $\sqrt{s} = 8$ TeV, Phys. Rev. D 90 (2014) 032008. 1404.4619 https://doi.org/10.1103/PhysRevD.90.032008
[7] CMS Collaboration, Observation of $WW\gamma$ production and search for $h\gamma$ production in proton–proton collisions at $\sqrt{s} = 13$ TeV, Phys. Rev. Lett. 132 (2024) 121901. 2310.05164 https://doi.org/10.1103/PhysRevLett.132.121901
[8] ATLAS Collaboration, Observation of WWW production in pp collisions at $\sqrt{s} = 13$ TeV with the ATLAS detector, Phys. Rev. Lett. 129 (2022) 061803. 2201.13045 https://doi.org/10.1103/PhysRevLett.129.061803
[9] CMS Collaboration, Observation of the production of three massive gauge bosons at $\sqrt{s} = 13$ TeV, Phys. Rev. Lett. 125 (2020) 151802. 2006.11191 https://doi.org/10.1103/PhysRevLett.125.151802
[10] ATLAS Collaboration, Observation of $W\gamma\gamma$ triboson production in proton–proton collisions at $\sqrt{s} = 13$ TeV with the ATLAS detector, Phys. Lett. B 848 (2024) 138400. 2308.03041 https://doi.org/10.1016/j.physletb.2023.138400
[11] CMS Collaboration, Measurements of the $pp \to W^{\pm}\gamma\gamma$ and $pp \to Z\gamma\gamma$ cross sections at $\sqrt{s} = 13$ TeV and limits on anomalous quartic gauge couplings, JHEP 10 (2021) 174. 2105.12780 https://doi.org/10.1007/JHEP10(2021)174
[12] ATLAS Collaboration, Measurement of $Z\gamma\gamma$ production in pp collisions at $\sqrt{s} = 13$ TeV with the ATLAS detector, Eur. Phys. J. C 83 (2023) 539. 2211.14171 https://doi.org/10.1140/epjc/s10052-023-11579-8
[13] ATLAS Collaboration, Observation of $WZ\gamma$ production in pp collisions at $\sqrt{s} = 13$ TeV with the ATLAS detector, Phys. Rev. Lett. 132 (2024) 021802. 2305.16994 https://doi.org/10.1103/PhysRevLett.132.021802
[14] CMS Collaboration, Observation of $WZ\gamma$ production and constraints on new physics scenarios in proton–proton collisions at $\sqrt{s} = 13$ TeV, Phys. Rev. D 112 (2025) 012009. 2503.21977 https://doi.org/10.1103/cm24-665b
[15] ATLAS Collaboration, Observation of VVZ production at $\sqrt{s} = 13$ TeV with the ATLAS detector, Phys. Lett. B 866 (2025) 139527. 2412.15123 https://doi.org/10.1016/j.physletb.2025.139527
[16] ATLAS Collaboration, Luminosity determination in pp collisions at $\sqrt{s} = 13$ TeV using the ATLAS detector at the LHC, Eur. Phys. J. C 83 (2023) 982. 2212.09379 https://doi.org/10.1140/epjc/s10052-023-11747-w
[17] O.J.P. Éboli, M.C. Gonzalez-Garcia, Classifying the bosonic quartic couplings, Phys. Rev. D 93(9) (2016) 093013. 1604.03555 https://doi.org/10.1103/PhysRevD.93.093013
[18] ATLAS Collaboration, The ATLAS Collaboration Software and Firmware, ATL-SOFT-PUB-2021-001 https://cds.cern.ch/record/2767187, 2021.
[19] ATLAS Collaboration, ATLAS data quality operations and performance for 2015–2018 data-taking, JINST 15 (2020) P04003. 1911.04632 https://doi.org/10.1088/1748-0221/15/04/P04003
[20] ATLAS Collaboration, Performance of the ATLAS trigger system in 2015, Eur. Phys. J. C 77 (2017) 317. 1611.09661 https://doi.org/10.1140/epjc/s10052-017-4852-3
[21] ATLAS Collaboration, Performance of electron and photon triggers in ATLAS during LHC run 2, Eur. Phys. J. C 80 (2020) 47. 1909.00761 https://doi.org/10.1140/epjc/s10052-019-7500-2
[22] S. Agostinelli, et al., GEANT4 – a simulation toolkit, Nucl. Instrum. Meth. A 506 (2003) 250. https://doi.org/10.1016/S0168-9002(03)01368-8
[23] ATLAS Collaboration, The ATLAS simulation infrastructure, Eur. Phys. J. C 70 (2010) 823. 1005.4568 https://doi.org/10.1140/epjc/s10052-010-1429-9
[24] T. Sjöstrand, S. Mrenna, P. Skands, A brief introduction to PYTHIA 8.1, Comput. Phys. Commun. 178 (2008) 852–867. 0710.3820 https://doi.org/10.1016/j.cpc.2008.01.036
[25] ATLAS Collaboration, The Pythia 8 A3 tune description of ATLAS minimum bias and inelastic measurements incorporating the Donnachie–Landshoff diffractive model, ATL-PHYS-PUB-2016-017 https://cds.cern.ch/record/2206965., 2016.
[26] NNPDF Collaboration, R.D. Ball, et al., Parton distributions with LHC data, Nucl. Phys. B 867 (2013) 244. 1207.1303 https://doi.org/10.1016/j.nuclphysb.2012.10.003
[27] E. Bothmann, et al., Event generation with sherpa 2.2, SciPost Phys. 7(3) (2019) 034. 1905.09127 https://doi.org/10.21468/SciPostPhys.7.3.034
[28] NNPDF Collaboration, R.D. Ball, et al., Parton distributions for the LHC run II, JHEP 04 (2015) 040. 1410.8849 https://doi.org/10.1007/JHEP04(2015)040
[29] T. Gleisberg, S. Höche, Comix, a new matrix element generator, JHEP 12 (2008) 039. 0808.3674 https://doi.org/10.1088/1126-6708/2008/12/039
[30] F. Buccioni, J.-N. Lang, J.M. Lindert, P. Maierhöfer, S. Pozzorini, H. Zhang, M.F. Zoller, OpenLoops 2, Eur. Phys. J. C 79(10) (2019) 866. 1907.13071 https://doi.org/10.1140/epjc/s10052-019-7306-2
[31] F. Cascioli, P. Maierhöfer, S. Pozzorini, Scattering amplitudes with open loops, Phys. Rev. Lett. 108 (2012) 111601. 1111.5206 https://doi.org/10.1103/PhysRevLett.108.111601
[32] A. Denner, S. Dittmaier, L. Hofer, COLLIER: a fortran-based complex one-loop library in extended regularizations, Comput. Phys. Commun. 212 (2017) 220–238. 1604.06792 https://doi.org/10.1016/j.cpc.2016.10.013
[33] S. Schumann, F. Krauss, A parton shower algorithm based on Catani–Seymour dipole factorisation, JHEP 03 (2008) 038. 0709.1027 https://doi.org/10.1088/1126-6708/2008/03/038
[34] S. Höche, F. Krauss, M. Schönherr, F. Siegert, A critical appraisal of NLO + PS matching methods, JHEP 09 (2012) 049. 1111.1220 https://doi.org/10.1007/JHEP09(2012)049
[35] S. Höche, F. Krauss, M. Schönherr, F. Siegert, QCD matrix elements + parton showers. the NLO case, JHEP 04 (2013) 027. 1207.5030 https://doi.org/10.1007/JHEP04(2013)027
[36] S. Catani, F. Krauss, B.R. Webber, R. Kuhn, QCD Matrix elements + parton showers, JHEP 11 (2001) 063. hep-ph/0109231 https://doi.org/10.1088/1126-6708/2001/11/063
[37] S. Höche, F. Krauss, S. Schumann, F. Siegert, QCD matrix elements and truncated showers, JHEP 05 (2009) 053. 0903.1219 https://doi.org/10.1088/1126-6708/2009/05/053
[38] J. Alwall, R. Frederix, S. Frixione, V. Hirschi, F. Maltoni, O. Mattelaer, H.S. Shao, T. Stelzer, P. Torrielli, M. Zaro, The automated computation of tree-level and next-to-leading order differential cross sections, and their matching to parton shower simulations, JHEP 07 (2014) 079. 1405.0301 https://doi.org/10.1007/JHEP07(2014)079
[39] T. Sjöstrand, S. Ask, J.R. Christiansen, R. Corke, N. Desai, P. Ilten, S. Mrenna, S. Prestel, C.O. Rasmussen, P.Z. Skands, An introduction to PYTHIA 8.2, Comput. Phys. Commun. 191 (2015) 159. 1410.3012 https://doi.org/10.1016/j.cpc.2015.01.024
[40] ATLAS Collaboration, ATLAS Pythia 8 tunes to 7 TeV data, ATL-PHYS-PUB-2014-021 https://cds.cern.ch/record/1966419, 2014.
[41] S. Frixione, E. Laenen, P. Motylinski, B.R. Webber, Angular correlations of lepton pairs from vector boson and top quark decays in Monte Carlo simulations, JHEP 04 (2007) 081. hep-ph/0702198 https://doi.org/10.1088/1126-6708/2007/04/081
[42] P. Artoisenet, R. Frederix, O. Mattelaer, R. Rietkerk, Automatic spin-entangled decays of heavy resonances in Monte Carlo simulations, JHEP 03 (2013) 015. 1212.3460 https://doi.org/10.1007/JHEP03(2013)015
[43] ATLAS Collaboration, Measurement of the charge asymmetry in top-quark pair production in association with a photon with the ATLAS experiment, Phys. Lett. B 843 (2023) 137848. 2212.10552 https://doi.org/10.1016/j.physletb.2023.137848
[44] S. Frixione, G. Ridolfi, P. Nason, A positive-weight next-to-leading-order Monte Carlo for heavy flavour hadroproduction, JHEP 09 (2007) 126. 0707.3088 https://doi.org/10.1088/1126-6708/2007/09/126
[45] P. Nason, A new method for combining NLO QCD with shower Monte Carlo algorithms, JHEP 11 (2004) 040. hep-ph/0409146 https://doi.org/10.1088/1126-6708/2004/11/040
[46] S. Frixione, P. Nason, C. Oleari, Matching NLO QCD computations with parton shower simulations: the POWHEG method, JHEP 11 (2007) 070. 0709.2092 https://doi.org/10.1088/1126-6708/2007/11/070
[47] S. Alioli, P. Nason, C. Oleari, E. Re, A general framework for implementing NLO calculations in shower Monte Carlo programs: the POWHEG BOX, JHEP 06 (2010) 043. 1002.2581 https://doi.org/10.1007/JHEP06(2010)043
[48] ATLAS Collaboration, Studies on top-quark Monte Carlo modelling for Top2016, ATL-PHYS-PUB-2016-020 https://cds.cern.ch/record/2216168, 2016.

[49] ATLAS Collaboration, Vertex Reconstruction Performance of the ATLAS Detector at $\sqrt{s} = 13$ TeV, ATL-PHYS-PUB-2015-026 https://cds.cern.ch/record/2037717, 2015.

[50] ATLAS Collaboration, Electron and photon performance measurements with the ATLAS detector using the 2015–2017 LHC proton–proton collision data, JINST 14 (2019) P12006. 1908.00005 https://doi.org/10.1088/1748-0221/14/12/P12006

[51] ATLAS Collaboration, Performance of the ATLAS track reconstruction algorithms in dense environments in LHC run 2, Eur. Phys. J. C 77 (2017) 673. 1704.07983 https://doi.org/10.1140/epjc/s10052-017-5225-7

[52] ATLAS Collaboration, Muon reconstruction and identification efficiency in ATLAS using the full run 2 pp collision data set at $\sqrt{s} = 13$ TeV, Eur. Phys. J. C 81 (2021) 578. 2012.00578 https://doi.org/10.1140/epjc/s10052-021-09233-2

[53] ATLAS Collaboration, Jet reconstruction and performance using particle flow with the ATLAS detector, Eur. Phys. J. C 77 (2017) 466. 1703.10485 https://doi.org/10.1140/epjc/s10052-017-5031-2

[54] M. Cacciari, G.P. Salam, G. Soyez, The anti-k_t jet clustering algorithm, JHEP 04 (2008) 063. 0802.1189 https://doi.org/10.1088/1126-6708/2008/04/063

[55] M. Cacciari, G.P. Salam, G. Soyez, FastJet user manual, Eur. Phys. J. C 72 (2012) 1896. 1111.6097 https://doi.org/10.1140/epjc/s10052-012-1896-2

[56] ATLAS Collaboration, Tagging and suppression of pileup jets with the ATLAS detector, ATLAS-CONF-2014-018 https://cds.cern.ch/record/1700870, 2014.

[57] ATLAS Collaboration, ATLAS B-jet identification performance and efficiency measurement with $t\bar{t}$ events in pp collisions at $\sqrt{s} = 13$ TeV, Eur. Phys. J. C 79 (2019) 970. 1907.05120 https://doi.org/10.1140/epjc/s10052-019-7450-8

[58] ATLAS Collaboration, Calibration of the light-flavour jet mistagging efficiency of the b-tagging algorithms with Z +jets events using 139 fb^{-1} of ATLAS proton–proton collision data at $\sqrt{s} = 13$ TeV, Eur. Phys. J. C 83 (2023) 728. 2301.06319 https://doi.org/10.1140/epjc/s10052-023-11736-z

[59] ATLAS Collaboration, ATLAS flavour-tagging algorithms for the LHC run 2 pp collision dataset, Eur. Phys. J. C 83 (2023) 681. 2211.16345 https://doi.org/10.1140/epjc/s10052-023-11699-1

[60] ATLAS Collaboration, Performance of missing transverse momentum reconstruction with the ATLAS detector using proton–proton collisions at $\sqrt{s} = 13$ TeV, Eur. Phys. J. C 78 (2018) 903. 1802.08168 https://doi.org/10.1140/epjc/s10052-018-6288-9

[61] ATLAS Collaboration, Search for flavour-changing neutral-current couplings between the top quark and the photon with the ATLAS detector at $\sqrt{s} = 13$ TeV, Phys. Lett. B 842 (2023) 137379. 2205.02537 https://doi.org/10.1016/j.physletb.2022.137379

[62] ATLAS Collaboration, Observation of single-top-quark production in association with a photon using the ATLAS detector, Phys. Rev. Lett. 131 (2023) 181901. 2302.01283 https://doi.org/10.1103/PhysRevLett.131.181901

[63] ATLAS Collaboration, Measurements of inclusive and differential cross-sections of $t\bar{t}\gamma$ production in pp collisions at $\sqrt{s} = 13$ TeV with the ATLAS detector, JHEP 10 (2024) 191. 2403.09452 https://doi.org/10.1007/JHEP10(2024)191

[64] S. Das, A simple alternative to the crystal ball function (2016). 1603.08591

[65] ATLAS Collaboration, Measurements of $Z\gamma$+jets differential cross sections in pp collisions at $\sqrt{s} = 13$ TeV with the ATLAS detector, JHEP 07 (2023) 072. 2212.07184 https://doi.org/10.1007/JHEP07(2023)072

[66] T. Chen, C. Guestrin, XGBoost: a scalable tree boosting system (2016). 1603.02754 https://doi.org/10.1145/2939672.2939785

[67] M. Stone, Cross-validatory choice and assessment of statistical predictions, J. R. Stat. Soc. Ser. B (Methodological) 36(2) (1974) 111–147. https://doi.org/10.1111/j.2517-6161.1974.tb00994.x

[68] G. James, et al., An Introduction to Statistical Learning: With Applications in R, Springer, New York, NY, 2013.

[69] ATLAS Collaboration, Jet energy scale and resolution measured in proton–proton collisions at $\sqrt{s} = 13$ TeV with the ATLAS detector, Eur. Phys. J. C 81 (2021) 689. 2007.02645 https://doi.org/10.1140/epjc/s10052-021-09402-3

[70] ATLAS Collaboration, Performance of pile-up mitigation techniques for jets in pp collisions at $\sqrt{s} = 8$ TeV using the ATLAS detector, Eur. Phys. J. C 76 (2016) 581. 1510.03823 https://doi.org/10.1140/epjc/s10052-016-4395-z

[71] ATLAS Collaboration, Measurement of the c-jet mistagging efficiency in $t\bar{t}$ events using pp collision data at $\sqrt{s} = 13$ TeV collected with the ATLAS detector, Eur. Phys. J. C 82 (2022) 95. 2109.10627 https://doi.org/10.1140/epjc/s10052-021-09843-w

[72] G. Avoni, et al., The new LUCID-2 detector for luminosity measurement and monitoring in ATLAS, JINST 13 (2018) P07017. https://doi.org/10.1088/1748-0221/13/07/P07017

[73] J. Butterworth, et al., PDF4LHC recommendations for LHC run II, J. Phys. G 43 (2016) 023001. 1510.03865 https://doi.org/10.1088/0954-3899/43/2/023001

[74] M. Aly, T. Dado, A. Held, M. Pinamonti, L. Valery, Trexfitter (2025). https://doi.org/10.5281/zenodo.15642614

[75] ROOT Collaboration, HistFactory: A tool for creating statistical models for use with RooFit and RooStats, Technical Report CERN-OPEN-2012-016, New York U., New York, 2012. https://cds.cern.ch/record/1456844.

[76] W. Verkerke, D. Kirkby, The RooFit toolkit for data modeling, 2003. physics/0306116

[77] A. Pinto, Z. Wu, F. Balli, N. Berger, M. Boonekamp, E. Chapon, T. Kawamoto, B. Malaescu, Uncertainty components in profile likelihood fits, Eur. Phys. J. C 84(6) (2024) 593. 2307.04007 https://doi.org/10.1140/epjc/s10052-024-12877-5

[78] G. Cowan, K. Cranmer, E. Gross, O. Vitells, Asymptotic formulae for likelihood-based tests of new physics, Eur. Phys. J. C 71 (2011) 1554. 1007.1727 https://doi.org/10.1140/epjc/s10052-011-1554-0

[79] ATLAS Collaboration, $ZZ \to \ell^+\ell^-\ell'^+\ell'^-$ Cross-section measurements and dummyTXdummy– search for anomalous triple gauge couplings in 13 TeV pp collisions with the ATLAS detector, Phys. Rev. D 97 (2018) 032005. 1709.07703 https://doi.org/10.1103/PhysRevD.97.032005

[80] ATLAS Collaboration, Measurement of ZZ production in the $\ell\ell\nu\nu$ final state with the ATLAS detector in pp collisions at $\sqrt{s} = 13$ TeV, JHEP 10 (2019) 127. 1905.07163 https://doi.org/10.1007/JHEP10(2019)127

[81] ATLAS Collaboration, Measurement of the $Z\gamma \to \nu\bar{\nu}\gamma$ production cross section in pp collisions at $\sqrt{s} = 13$ TeV with the ATLAS detector and limits on anomalous triple gauge-boson couplings, JHEP 12 (2018) 010. 1810.04995 https://doi.org/10.1007/JHEP12(2018)010

[82] ATLAS Collaboration, Measurement of fiducial and differential W^+W^- production cross-sections at $\sqrt{s} = 13$ TeV with the ATLAS detector, Eur. Phys. J. C 79 (2019) 884. 1905.04242 https://doi.org/10.1140/epjc/s10052-019-7371-6

[83] CMS Collaboration, Measurements of the $pp \to ZZ$ production cross section and the $Z \to 4\ell$ branching fraction, and constraints on anomalous triple gauge couplings at $\sqrt{s} = 13$ TeV, Eur. Phys. J. C 78 (2018) 165. 1709.08601 https://doi.org/10.1140/epjc/s10052-018-5567-9

[84] CMS Collaboration, Electroweak production of two jets in association with a Z boson in proton–proton collisions at $\sqrt{s} = 13$ TeV, Eur. Phys. J. C 78 (2018) 589. 1712.09814 https://doi.org/10.1140/epjc/s10052-018-6049-9

[85] CMS Collaboration, Measurement of electroweak production of a W boson in association with two jets in proton–proton collisions at $\sqrt{s} = 13$ TeV, Eur. Phys. J. C 80 (2020) 43. 1903.04040 https://doi.org/10.1140/epjc/s10052-019-7585-7

[86] CMS Collaboration, Measurements of the $pp \to WZ$ inclusive and differential production cross sections and constraints on charged anomalous triple gauge couplings at $\sqrt{s} = 13$ TeV, JHEP 04 (2019) 122. 1901.03428 https://doi.org/10.1007/JHEP04(2019)122

[87] CMS Collaboration, W^+W^- boson pair production in proton–proton collisions at $\sqrt{s} = 13$ TeV, Phys. Rev. D 102 (2020) 092001. 2009.00119 https://doi.org/10.1103/PhysRevD.102.092001

[88] CMS Collaboration, Search for anomalous triple gauge couplings in WW and WZ production in lepton + jet events in proton–proton collisions at $\sqrt{s} = 13$ TeV, JHEP 12 (2019) 062. 1907.08354 https://doi.org/10.1007/JHEP12(2019)062

[89] CMS Collaboration, Measurements of $pp \to ZZ$ production cross sections and constraints on anomalous triple gauge couplings at $\sqrt{s} = 13$ TeV, Eur. Phys. J. C 81 (2021) 200. 2009.01186 https://doi.org/10.1140/epjc/s10052-020-08817-8

[90] S.S. Wilks, The large-sample distribution of the likelihood ratio for testing composite hypotheses, Annals Math. Statist. 9(1) (1938) 60–62. https://doi.org/10.1214/aoms/1177732360

[91] ATLAS Collaboration, Fiducial and differential cross-section measurements of electroweak $W\gamma jj$ production in pp collisions at $\sqrt{s} = 13$ TeV with the ATLAS detector, Eur. Phys. J. C 84 (2024) 1064. 2403.02809 https://doi.org/10.1140/epjc/s10052-024-13311-6

[92] I. Brivio, et al., Truncation, validity, uncertainties (2022). 2201.04974

[93] E.d.S. Almeida, O.J.P. Éboli, M.C. Gonzalez-Garcia, Unitarity constraints on anomalous quartic couplings, Phys. Rev. D 101(11) (2020) 113003. 2004.05174 https://doi.org/10.1103/PhysRevD.101.113003

[94] ATLAS Collaboration, ATLAS Computing Acknowledgements, ATL-SOFT-PUB-2025-001 https://cds.cern.ch/record/2922210, 2025.